

## ABSTRACT

### Analytic Modeling and Applications of Barotropic Flows over Sloping Topographies Using Similarity Solutions

Ruy Ibanez Amador, M.S.M.E

Chairperson: Joseph Kuehl, Ph.D.

The continental slope is a region in the ocean that consists of a strong sloping topography. The slope acts as a barrier to large scale geophysical transport, but small scale mechanisms are not well understood. Studies are mostly limited to large scale simulations and spatially limited field measurements. I developed an analytic method to obtain a base flow field for regions of the continental slope. Using scaling arguments, I reduce the system to the leading order dynamical balances and apply a similarity method to find solutions of the flow. It is possible to retain the nonlinear terms for a special case, which provides insight into the base nonlinear dynamics of the flow. I show that the solutions are relevant to regions of the continental slope using bathymetry data from the National Oceanic and Atmospheric Administration.

Analytic Modeling and Applications of Barotropic Flows over Sloping Topographies  
Using Similarity Solutions

by

Ruy Ibanez Amador, B.S.

A Thesis

Approved by the Department of Mechanical Engineering

---

Kenneth Van Treuren, Ph.D., Interim Chairperson

Submitted to the Graduate Faculty of  
Baylor University in Partial Fulfillment of the  
Requirements for the Degree  
of  
Master of Science in Mechanical Engineering

Approved by the Thesis Committee

---

Joseph Kuehl, Ph.D., Chairperson

---

Stephen McClain, Ph.D.

---

John Dunbar, Ph.D.

Accepted by the Graduate School  
May 2017

---

J. Larry Lyon, Ph.D., Dean



## TABLE OF CONTENTS

LIST OF FIGURES .....	vi
DEDICATION .....	vii
CHAPTER ONE	
Introduction .....	1
<i>Motivation</i> .....	2
CHAPTER TWO	
A Mathematical Description of the Ocean .....	3
<i>Scale Analysis of the Ocean</i> .....	3
<i>The Equations of Motion</i> .....	5
<i>Coriolis Effect</i> .....	5
<i>The Sloping Bottom and Continuity Equation</i> .....	10
<i>Vorticity Equations</i> .....	11
<i>The Ekman Layer</i> .....	13
<i>Final Equations</i> .....	15
<i>Vorticity-Transport Equation</i> .....	16
<i>Similarity Solutions</i> .....	18
CHAPTER THREE	
Solutions to the Model Equations .....	20
<i>Expanding Jet Solution</i> .....	20
<i>Compressing Jet Solution</i> .....	23
<i>Extension of Solutions</i> .....	29
CHAPTER FOUR	
Applications .....	33
<i>Examples</i> .....	35
CHAPTER FIVE	
Conclusion .....	40
<i>Summary</i> .....	40
<i>Future Work</i> .....	40
APPENDIX A	
Lambert W function .....	43
APPENDIX B	
Matlab Code .....	44

APPENDIX C	
MATLAB - .xyz Reader .....	49
APPENDIX D	
MATLAB - Orthogonal Line Procedure .....	50
APPENDIX E	
MATLAB - Fitting.....	54
BIBLIOGRAPHY .....	60

## LIST OF FIGURES

Figure 1.1 Sections of the Ocean .....	1
Figure 2.1 Florida Coast Topography Surface Plot.....	3
Figure 2.2 Simplified Domain .....	4
Figure 2.3 Spherical Earth Domain .....	6
Figure 2.4 Rotating Frame .....	6
Figure 2.5 Sloping and No Penetration Condition.....	11
Figure 2.6 Conservation of Potential Vorticity.....	12
Figure 3.1 Expanding Jet Domain.....	21
Figure 3.2 Linear Flow Field.....	24
Figure 3.3 Compressing Jet Domain .....	25
Figure 3.4 Nonlinear Parameter Comparison .....	30
Figure 3.5 Compressing Jet Flow Field .....	31
Figure 4.1 Florida Coast .....	36
Figure 4.2 Florida Coast Slope .....	37
Figure 4.3 Florida Coast Flow Field.....	37
Figure 4.4 Norway Coast .....	38
Figure 4.5 Norway Coast Slope .....	39
Figure 4.6 Norway Coast Flow Field .....	39

## DEDICATION

To my family and advisors for their endless support

## CHAPTER ONE

### Introduction

In this work I present an analytic model for oceanographic flows over a sloping topography. There are various regions in the ocean for which this model is valid. I will focus on the continental slope, which is a section in the ocean that has a strong slope and connects the outer edge of the continental shelf to the deep ocean floor. Figure 1.1 is a diagram that shows different sections of the ocean's topography, including the continental slope.

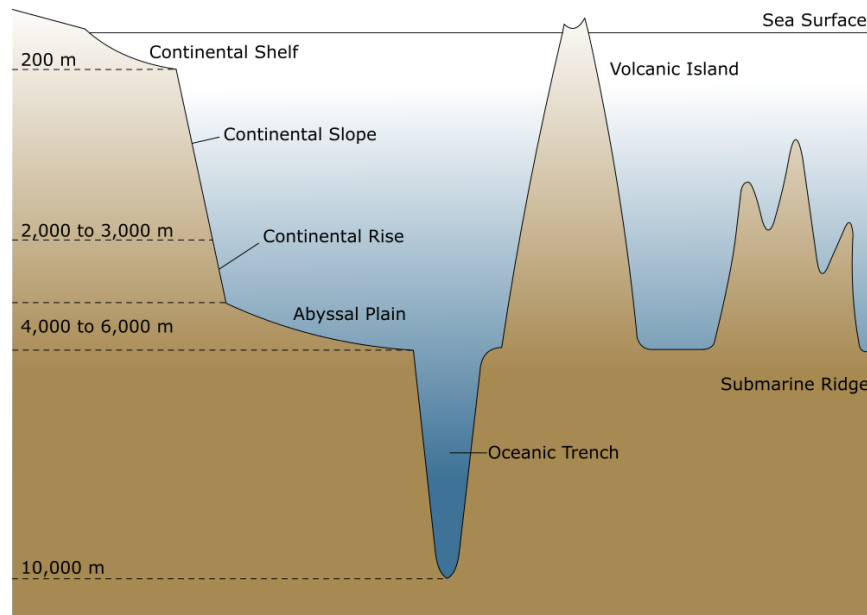


Figure 1.1. Source: Wikimedia Commons

The scale of the ocean causes flows to behave in a manner that differs from everyday flows we observe outside boundary layers. The large size of the ocean causes viscous effects to be of little importance. In addition the rotation of the Earth, imparts a condition for currents to conserve their depth. In other words, a parcel of



fluid will tend to follow along topographic features. This phenomena is formalized in the statement of conservation of potential vorticity, which is a consequence of the Earth’s rotation. This suggests that the continental slope acts as a barrier of material transport between the outer edge of the continental shelf and the deep ocean floor.

### *Motivation*

Ocean currents play an important role in various phenomena across multiple disciplines, such as climate science, weather science, marine science, energy, etc. The scale and complexity of the ocean make it very difficult to model using simple methods. The most commonly used methods for studying ocean currents are observational programs and/or numerical simulations. These methods are resource intensive, and thus can only provide limited results. Observations (Maier et al., 2016) require expensive equipment and have limited range in their data sampling. Computational models (Nguyen, Morey, Dukhovskoy, & Chassignet, 2015) require large amounts of computational power and suffer from imperfect understanding of flow initial conditions, flow parameters and physics. In this work, I present an analytic mathematical method to model large scale ocean flows with a sloping topography. My results can be used to model the regions analyzed in the previously cited studies, but with minimal resources. The transport mechanisms around the continental slope of materials (Maier et al., 2016), energy (Jia Wang, 2003) and wildlife (John, Mittelstaedt, & Schulz, 1998) are not well understood. Studies are limited in resources and have been focused away from understanding the base physics of the phenomenon. My analytic model opens the possibility to study transport around the continental slope using analytic Lagrangian methods. It can also help develop better numerical models by providing a low order approximation for initialization of numerical simulations.

## CHAPTER TWO

### A Mathematical Description of the Ocean

In this chapter I derive a mathematical description of the ocean. Using scaling analysis I determine the relevant equations which model the dynamics of geophysical flows over the continental slope. I also provide an introduction to the mathematical techniques that I use to solve the final system of equations.

#### *Scale Analysis of the Ocean*

In the continental slope, the bottom topography has a strong slope that connects the continental shelf to the abyssal ocean. I am interested in constructing a mathematical description of this sloping region. Figure 2.1 is a surface plot of topographic data near the Florida coast. It is easy to visually identify the continental slope due to its rapid change in depth, relative to the size of the ocean.

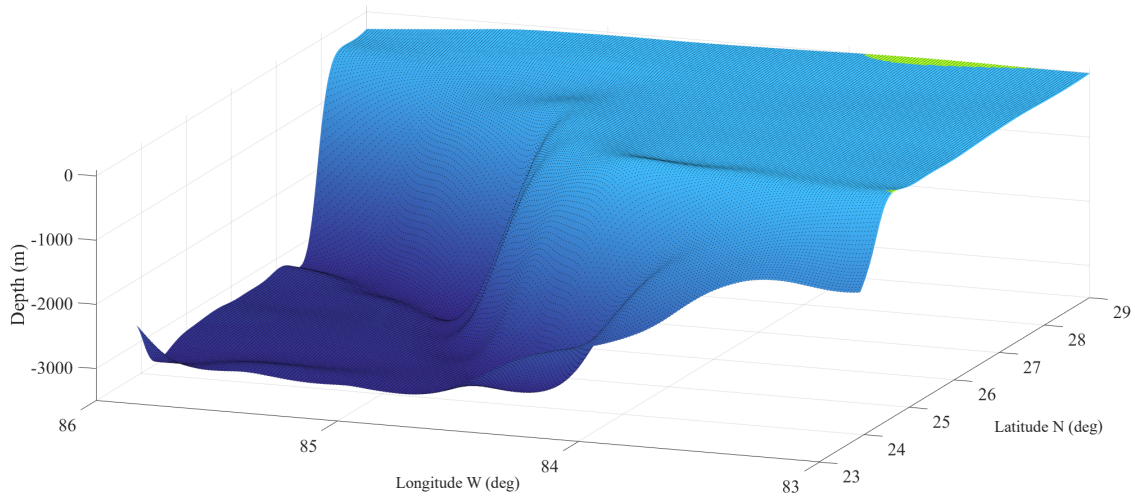


Figure 2.1: Surface plot of the ocean topography near the Florida coast. The green region indicates land.

I can reduce the complex features of real world topographies to determine the dominant components. In essence, I am simplifying the domain to an idealized description based on the scaling arguments. Figure 2.2 is a sketch of what the simplified domain may look like and indicates the dominant scales that were taken into account. While the figure shows a linear, ramp-like topography, it is not limited to that specific shape.

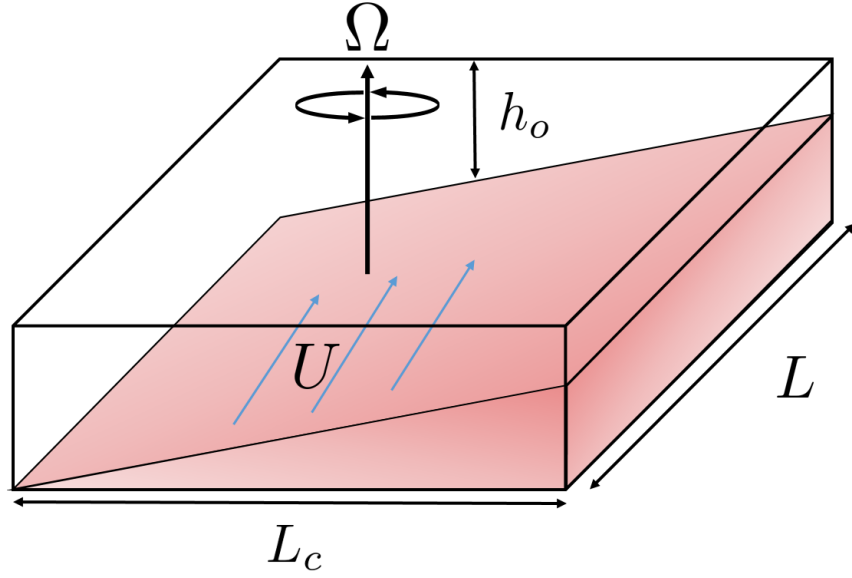


Figure 2.2: Sketch of the domain.  $U$  is the stream velocity scale,  $\Omega$  is the frame rotation scale,  $h_o$  is the depth scale,  $L$  is the downstream length scale and  $L_c$  is the cross-stream length scale.

Typical length scales for sections of the continental slope are

Downstream length scale  $L$ :  $\mathcal{O}(10^5)$  m

Cross-stream length scale  $L_c$ :  $\mathcal{O}(10^3)$  m

Depth length scale  $h_o$ :  $\mathcal{O}(10^3)$  m

Stream velocity scale  $U$ :  $\mathcal{O}(10^{-1})$  m/s

Rotational scale  $\Omega$ :  $\mathcal{O}(10^{-4})$  rad/s

Viscosity scale  $\nu$ :  $\mathcal{O}(10^{-6})$  m<sup>2</sup>/s

### *The Equations of Motion*

Based on the scales for the problem, I now seek the equations that describe the fluid motion. I start with the Navier-Stokes equations in vector form ( $U = (u, v, w)$ ) with no external forces (equation 2.1) and the continuity equation (equation 2.2).

$$\frac{\partial U}{\partial t} + U \cdot \nabla U = -\frac{\nabla P}{\rho} + \nu \nabla^2 U \quad (2.1)$$

$$\frac{\partial \rho}{\partial t} + \frac{\partial \rho u}{\partial x} + \frac{\partial \rho v}{\partial y} + \frac{\partial \rho w}{\partial z} = 0 \quad (2.2)$$

The first assumption I make is that the fluid is homogeneous and incompressible, in other words, density is constant. This is known as the barotropic approximation. The continuity equation then takes the following form

$$\frac{\partial u}{\partial x} + \frac{\partial v}{\partial y} + \frac{\partial w}{\partial z} = 0 \quad (2.3)$$

### *Coriolis Effect*

In geophysical flows the Coriolis effect, caused by the Earth's rotation, has an important role in the dynamics. The domain is a small inertial frame on the large rotating body that is the earth. Figure 2.3 is a sketch of the domain on the rotating spherical earth. To determine the influence of the rotating frame on the dynamics, I must modify the Navier-Stokes equations by transforming to a rotating frame. I find that additional terms are introduced into the Navier-Stokes equations.

Consider a rotating frame whose rotation is defined by the vector  $\Omega$ , which is constant and a position vector of constant magnitude  $A$ . The position vector  $A$  is in

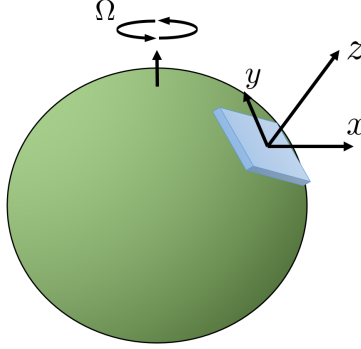


Figure 2.3: A sketch of the Earth as a sphere and the domain of our problem. The Earth's rotation is defined by the vector  $\Omega$ .

the rotating frame. The velocity of  $A$  is given by  $\Omega \times A = (\frac{dA}{dt})_I$ , where the subscript  $I$  denotes the velocity defined from the fixed frame.

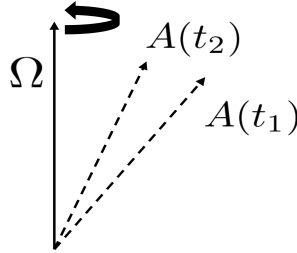


Figure 2.4. Vector  $A$  on a rotating frame with a rotation vector  $\Omega$

Now consider an arbitrary (not necessarily constant) vector  $B$  in a rotating frame. If I perform the same transformation, then the velocity of the vector in the fixed frame is given by  $(\frac{dB}{dt})_I = (\frac{dB}{dt})_R + \Omega \times B$  where the  $I$  subscript represents the fixed frame and  $R$  is the rotating frame. With this transformation I can implement the rotating frame effects into the Navier-Stokes equations.

The change in velocity of a parcel of fluid in the rotating frame is described by

$$U_I = U_R + \Omega \times R \quad (2.4)$$

where  $U_I$  is the velocity in the fixed frame,  $R$  is the position and  $U_R$  is the velocity in the rotating frame

Applying the same transformation again to equation 2.4 gives

$$\left(\frac{dU_I}{dt}\right)_I = \left(\frac{dU_I}{dt}\right)_R + \Omega \times U_I \quad (2.5)$$

which can be rewritten as

$$\left(\frac{dU_I}{dt}\right)_I = \left(\frac{dU_R}{dt}\right)_R + \frac{d\Omega}{dt} \times R + \Omega \times \left(\frac{dR}{dt}\right)_R + \Omega \times (U_R + \Omega \times R) \quad (2.6)$$

Note that the time derivative of  $\Omega$  is zero, since the rotation of the earth is constant, so it simplifies to

$$\left(\frac{dU_I}{dt}\right)_I = \left(\frac{dU_R}{dt}\right)_R + 2\Omega \times U_R + \Omega \times (\Omega \times R) \quad (2.7)$$

There are two added terms in the final equation.  $2\Omega \times U_R$  is the Coriolis acceleration and  $\Omega \times (\Omega \times R)$  the centrifugal acceleration. So, introducing the rotational effects into the Navier-Stokes equations gives

$$\frac{\partial U}{\partial t} + U \cdot \nabla U = -\frac{\nabla P}{\rho} + \nu \nabla^2 U - 2\Omega \times U - \Omega \times (\Omega \times R) \quad (2.8)$$

The method I used to arrive at this equation is the same procedure presented in Pedlosky (1979).

Let us analyze the centrifugal term  $\Omega \times (\Omega \times R)$ . The centrifugal force is parallel to that of gravity, and the order of magnitude of the centrifugal force  $\Omega^2 R_{earth} \approx 10^{-4}$  is much smaller compared to that of gravity. Thus, it is possible to neglect the centrifugal force. This is standard in the study of geophysical flows, as the centrifugal term rarely is of a relevant magnitude.

Now I perform scale analysis to determine the dominant components of the equations and further simplify our model. Let us first write the Navier-Stokes equation

in a scaled form. As an example of scaled form of  $\frac{\partial u}{\partial x}$  is  $\frac{U}{L}$ , this means that the order of magnitude of the partial derivative of the velocity over space will be approximately of the order of the velocity scale over the length scale. Applying this to equation 2.8 and neglecting the centrifugal term gives

$$\left[\frac{U}{T}\right] + \left[\frac{U^2}{L}\right] = -\left[\frac{P}{\rho L}\right] + \left[\nu \frac{U}{L^2}\right] - [2\Omega U] \quad (2.9)$$

I choose to neglect the time dependent term, as I am interested in finding steady solutions to the base flow. Thus, only the advective acceleration is retained. By multiplying by  $\frac{L}{U^2}$  I obtain the scale of the right hand terms relative to the advective acceleration.

$$1 = -\left[\frac{P}{\rho U^2}\right] + \left[\frac{\nu}{UL}\right] - \left[2\frac{\Omega L}{U}\right] \quad (2.10)$$

Plugging in typical scales for the ocean gives

$$\mathcal{O}(1) = -\left[\frac{P}{\rho U^2}\right] + \mathcal{O}(10^{-9}) - \mathcal{O}(10^2) \quad (2.11)$$

The Coriolis term scales inversely to the order of  $\frac{U}{\Omega L} \approx 10^{-2}$ , this number is called the Rossby number  $Ro$ . Since the inverse of the Rossby number is big in 2.11, the dominant term in the equations is the Coriolis term. Also, note that the viscosity term is very small, it scales with the inverse Reynolds number  $Re = \frac{UL}{\nu}$ . This means that the viscous forces play a small role in the interior flow dynamics.

It is important to emphasize the spherical geometry of the Earth. The domain is a Cartesian box on the surface of a spherical rotating frame, as seen in figure 2.3. The domain is defined in such a way that the  $x$ ,  $y$  and  $z$  axis represent east-west, north-south and up-down respectively. I have to project the rotation vector  $\Omega$  to the Cartesian domain, giving  $\Omega = (0, |\Omega|\cos\phi, |\Omega|\sin\phi)$ , where  $\phi$  is the azimuthal angle (latitude).

The Coriolis force acts using a cross product on the velocity. Thus, splitting this term by component gives the following Coriolis accelerations components

$$a_x = w\Omega_y - v\Omega_z \quad (2.12)$$

$$a_y = -w\Omega_x + u\Omega_z \quad (2.13)$$

$$a_z = v\Omega_x - u\Omega_y \quad (2.14)$$

where each subscript denotes the dimensional component. Note that  $\Omega_x = 0$  and in the context of ocean flows, the vertical components of the velocity and Coriolis acceleration are very small. Thus, I simplify the Coriolis accelerations to

$$a_x = -v\Omega_z \quad (2.15)$$

$$a_y = u\Omega_z \quad (2.16)$$

$$a_z = 0 \quad (2.17)$$

With these approximations I can now express the Earth's rotation effects on the Navier-Stokes equations with a single constant  $f = 2|\Omega|\sin\phi$ . Now that I have determined the dominant Coriolis terms, I analyze the effects on the dynamics by studying a dominated Coriolis flow, thus all terms are dropped from Navier-Stokes except for pressure and the Coriolis force

$$-fv = -\frac{\partial P}{\partial x} \quad (2.18)$$

$$fu = -\frac{\partial P}{\partial y} \quad (2.19)$$

$$0 = -\frac{\partial P}{\partial z} \quad (2.20)$$

This approximation shows that the pressure gradient in the vertical direction is 0, which suggests that the vertical velocity is constant and approximately 0, which



is consistent with the assumptions I made earlier. The two dimensional flow is balanced by pressure gradients. This approximation is called "geostrophic flow" and demonstrates some of the special characteristics in dynamics in ocean flows.

### *The Sloping Bottom and Continuity Equation*

Since I have assumed that the flow has constant density and is incompressible, the continuity equation is defined as  $\nabla \cdot U = 0$ . However, I must take into account that the model has a sloping bottom. The bottom is impenetrable which adds another condition that must be satisfied. The sloping bottom will force fluid to move in the vertical direction as shown in figure 2.5. I can describe the induced vertical velocity as

$$w = u \frac{\partial b}{\partial x} + v \frac{\partial b}{\partial y} \quad (2.21)$$

Recall from the geostrophic balance that  $w = 0$ , thus the continuity equation can take the form

$$u \frac{\partial b}{\partial x} + v \frac{\partial b}{\partial y} = 0 \quad (2.22)$$

The result is that the flow aligns itself with isobaths, even in the presence of obstacles, the flow will go around to preserve the same fluid thickness.

Now let us consider a more general case where  $w \neq 0$ . I can integrate the continuity equation  $\nabla \cdot U$  with respect to  $z$  since the horizontal velocities are independent of  $z$ .

$$\left( \frac{\partial u}{\partial x} + \frac{\partial v}{\partial y} \right) \int_b^{b+h} dz + [w]_b^{b+h} = 0 \quad (2.23)$$

Solving for  $w$  at each limit and combining gives

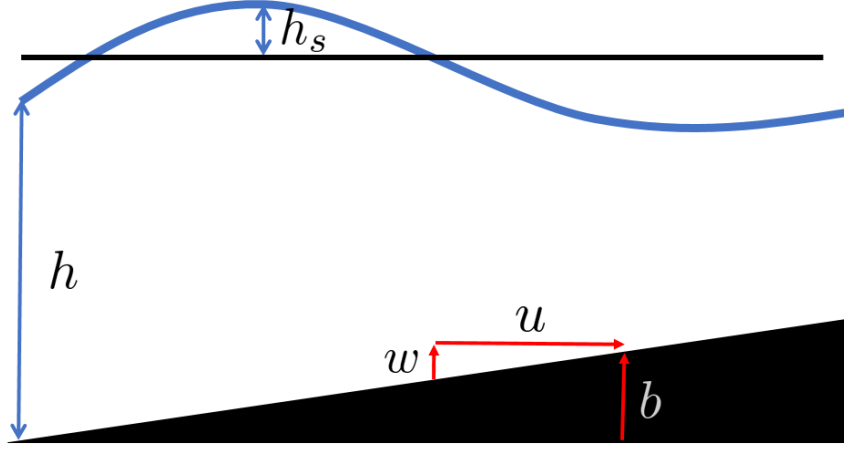


Figure 2.5: The bottom elevation is defined by  $b$ ,  $h$  is the depth, the surface elevation is defined as  $h_s$ , which are displacements of the fluid top boundary from a reference height  $H$ .

$$\frac{\partial h_s}{\partial t} + \frac{\partial hu}{\partial x} + \frac{\partial hv}{\partial y} = 0 \quad (2.24)$$

Where  $h_s = h + b - H$ . The convenient aspect of this new continuity equation is that the dependency on  $w$  has been eliminated by introducing a layer transport dependent on  $hu$  and  $hv$ .

### *Vorticity Equations*

The definition of relative vorticity is  $\omega = \frac{\partial v}{\partial x} - \frac{\partial u}{\partial y}$ . Let us explore how adding the rotational effects change the vorticity equation of the model system. It was established that the Coriolis force plays an important role, because of this the flow becomes flattened about the plane orthogonal to the rotation vector as shown in equations 2.18 to 2.20. In that approximation I neglected all components of the acceleration for simplification purposes, but to understand the effects on the vorticity I retain the acceleration terms, giving the following set of equations

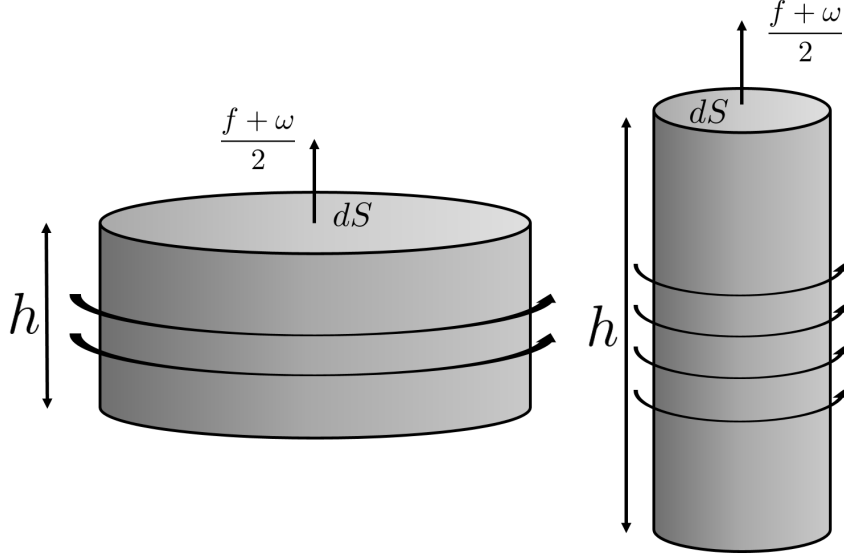


Figure 2.6: The image shows two columns of equivalent potential vorticity. Conservation is achieved by stretching and compressing the rotating column.

$$\frac{du}{dt} - fv = -\frac{\partial P}{\partial x} \quad (2.25)$$

$$\frac{dv}{dt} + fu = -\frac{\partial P}{\partial y} \quad (2.26)$$

$$0 = -\frac{\partial P}{\partial z} \quad (2.27)$$

Where  $\frac{d}{dt}$  is the material derivative  $\frac{\partial}{\partial t} + u\frac{\partial}{\partial x} + v\frac{\partial}{\partial y}$

Taking the curl of the equations gives

$$\frac{d}{dt}\left(f + \frac{\partial v}{\partial x} - \frac{\partial u}{\partial y}\right) + \left(\frac{\partial u}{\partial x} + \frac{\partial v}{\partial y}\right)\left(f + \frac{\partial v}{\partial x} - \frac{\partial u}{\partial y}\right) = 0 \quad (2.28)$$

which can be rewritten as

$$\frac{d}{dt}(f + \omega) + \left(\frac{\partial u}{\partial x} + \frac{\partial v}{\partial y}\right)(f + \omega) = 0 \quad (2.29)$$

Equation 2.29 shows that the vorticity equation includes the constant planetary vorticity  $f$  in addition the relative vorticity. To better illustrate the consequences of

this, consider a column of fluid whose cross-section is given by  $dS$  and height by  $h$ . Because the fluid is incompressible, it is possible to write conservation of volume as

$$\frac{d}{dt}(h dS) = 0 \quad (2.30)$$

Assuming  $h$  is constant over  $dS$ , I rewrite using equation 2.23 as

$$\frac{d}{dt}dS = \left(\frac{\partial u}{\partial x} + \frac{\partial v}{\partial y}\right)dS \quad (2.31)$$

This shows that a column of fluid under the influence of a rotating frame tends to expand and reduce its height or contract and increase its height. Looking back at the vorticity equation 2.29 one can start noticing similarities with 2.31. Combining equations 2.28 and 2.31 gives

$$\frac{d}{dt}(f + \omega)dS = 0 \quad (2.32)$$

then combining 2.30 and 2.32 yields

$$\frac{d}{dt}\left(\frac{f + \omega}{h}\right) = 0 \quad (2.33)$$

The equation shows that the quantity  $\frac{f + \omega}{h}$  has to be conserved. This quantity is called the potential vorticity  $q$  and will be useful for our analysis later.

### *The Ekman Layer*

In the scale analysis I determined that the viscosity term plays a small role on the dynamics, because the order of the viscous term in the Navier-Stokes equations is small. The viscous scaling parameters in equation 2.10 are equivalent to the inverse Reynolds number  $Re$ . In our problem  $Re = \frac{UL}{\nu} \approx 500$ . Typical fluid analysis suggests that the viscous forces in the flow are negligible compared to the inertial forces. However, if the viscous forces are neglected, information about the dynamics near the boundary layer would be lost.

I use a modified viscosity called Eddy viscosity  $\nu_E$ . The order of the eddy viscosity is much greater than the molecular viscosity  $\approx 10^{-2}$ . I calculate the Ekman number which is the ratio of the viscous forces to the Coriolis forces.

$$Ek = \frac{\nu_E}{\Omega H^2} \approx 10^{-4} \quad (2.34)$$

The Ekman number is small, which suggests that the vertical shear plays a small role in the interior flow equations. As I mentioned previously, it is not possible to neglect the viscous effects close to the bottom boundary, so I calculate the length where the viscosity is relevant with  $d = \sqrt{\frac{\nu_E}{f}}$ . This region of which is dominated by the viscous effects in a rotating fluid is called the Ekman layer, which is an analog to boundary layers in other fluid mechanics studies.

Following the approach in Cushman-Roisin and Beckers (2008), let us analyze the flow in the Ekman layer using the Navier-Stokes equations

$$-f(v - \bar{v}) = \nu_E \frac{\partial^2 u}{\partial^2 z} \quad (2.35)$$

$$f(u - \bar{u}) = \nu_E \frac{\partial^2 v}{\partial^2 z} \quad (2.36)$$

Note the flow equations are composed of two parts, the interior flow which is defined by  $\bar{u}$  and  $\bar{v}$ , and the flow near the bottom which is described by  $u$  and  $v$ . Note that the interior flow fields are constant with  $z$ . The boundary conditions for this problem are

$$u(z = 0) = 0 \quad (2.37)$$

$$v(z = 0) = 0 \quad (2.38)$$

$$u(z = \infty) = \bar{u} \quad (2.39)$$

$$v(z = \infty) = \bar{v} \quad (2.40)$$

The solution to these equations is

$$u = \bar{u} + e^{-\frac{z-b}{d}} \left( A \cos\left(\frac{z-b}{d}\right) + B \sin\left(\frac{z-b}{d}\right) \right) \quad (2.41)$$

$$v = \bar{v} + e^{-\frac{z-b}{d}} \left( B \cos\left(\frac{z-b}{d}\right) - A \sin\left(\frac{z-b}{d}\right) \right) \quad (2.42)$$

Where  $A$  and  $B$  are constants that are determined by the boundary conditions (no slip and interior flow),  $b$  is the height terrain elevation and  $d$  is the Ekman layer thickness. From the continuity equation, note that there is a non-zero divergence

$$w = \frac{d}{2} \left( \frac{\partial v}{\partial x} - \frac{\partial u}{\partial y} \right) \quad (2.43)$$

thus there is an Ekman suction which is given by

$$\nabla \cdot \Pi_E = -\frac{d}{2} \left( \frac{\partial v}{\partial x} - \frac{\partial u}{\partial y} \right) \quad (2.44)$$

### *Final Equations*

Note that from this point forward all subscripts of  $t$ ,  $x$  and  $y$  represent partial derivatives. For example  $(\frac{4f}{k})_x = \frac{\partial}{\partial x}(\frac{4f}{k})$ . Beginning with the following equations of motion for the model:

$$u_t + u \frac{\partial u}{\partial x} + v \frac{\partial u}{\partial y} - f v = -\frac{1}{\rho} \frac{\partial P}{\partial x} + \nu \frac{\partial^2 u}{\partial x^2} + \nu \frac{\partial^2 u}{\partial y^2} + \nu \frac{\partial^2 u}{\partial z^2} \quad (2.45)$$

$$v_t + u \frac{\partial v}{\partial x} + v \frac{\partial v}{\partial y} + f u = -\frac{1}{\rho} \frac{\partial P}{\partial y} + \nu \frac{\partial^2 v}{\partial x^2} + \nu \frac{\partial^2 v}{\partial y^2} + \nu \frac{\partial^2 v}{\partial z^2} \quad (2.46)$$

$$\frac{\partial h_s}{\partial t} + \frac{\partial h u}{\partial x} + \frac{\partial h v}{\partial y} + \nabla \cdot \Pi_E = 0 \quad (2.47)$$

At this point it is convenient to rewrite the equations in such a way that includes a kinetic energy term  $e = u^2 + v^2$  and letting  $p = \frac{P}{\rho}$ .

$$u_t - (f + \frac{\partial v}{\partial x} - \frac{\partial u}{\partial y})v = -(p - e)_x + \nu \nabla^2 u \quad (2.48)$$

$$v_t + (f + \frac{\partial v}{\partial x} - \frac{\partial u}{\partial y})u = -(p - e)_y + \nu \nabla^2 v \quad (2.49)$$

$$\frac{\partial h_s}{\partial t} + \frac{\partial hu}{\partial x} + \frac{\partial hv}{\partial y} + \nabla \cdot \Pi_E = 0 \quad (2.50)$$

These equations will be the foundation of my analysis, Kuehl and Sheremet (2014) and Kuehl (2014).

### *Vorticity-Transport Equation*

Equations 2.48 to 2.50 describe the barotropic dynamics of geophysical flows. To further simplify the problem, I can reduce the number of equations by taking the curl of the momentum equations. In other words, I take the partial derivative with respect to  $x$  for the equation of  $v$  and subtract the partial derivative with respect to  $y$  of  $u$ , giving the following equation

$$\omega_t + \frac{\partial}{\partial y}((f + \frac{\partial v}{\partial x} - \frac{\partial u}{\partial y})v) + \frac{\partial}{\partial x}((f + \frac{\partial v}{\partial x} - \frac{\partial u}{\partial y})u) = -(p - e)_{xy} + (p - e)_{xy} + \nu \nabla^2 \omega \quad (2.51)$$

The energy and pressure terms cancel, reducing to

$$\omega_t + \frac{\partial}{\partial y}((f + \omega)v) + \frac{\partial}{\partial x}((f + \omega)u) = \nu \nabla^2 \omega \quad (2.52)$$

Rewriting this equation by multiplying the inner terms by  $\frac{h}{h}$  gives

$$\omega_t + \frac{\partial}{\partial y}(\frac{(f + \omega)}{h}hv) + \frac{\partial}{\partial x}(\frac{(f + \omega)}{h}hu) = \nu \nabla^2 \omega \quad (2.53)$$

Note that the terms inside the derivatives are the potential vorticity  $q = \frac{(f + \omega)}{h}$ . So, I rewrite this equation using a transport function  $\psi(x, y)$ , which is defined as  $\psi_x = hv$  and  $\psi_y = -hu$

$$\omega_t + \frac{\partial}{\partial y}(q\psi_x) - \frac{\partial}{\partial x}(q\psi_y) = \nu \nabla^2 \omega \quad (2.54)$$

It is possible to rewrite this equation in the more compact form

$$\omega_t + J(\psi, q) = q(h)_t - q \frac{d}{2} \omega + \nu \nabla^2 \omega \quad (2.55)$$

Where  $J(\psi, \omega)$  is the Jacobian of the equation defined as

$$J(\psi, q) = q_y \psi_x - q_x \psi_y \quad (2.56)$$

Also note

$$q(h)_t - q \frac{d}{2} \omega = q(\psi_{xy} - \psi_{yx}) \quad (2.57)$$

I introduced through the definition of the continuity equation and by substituting terms, an Ekman suction term  $-q \frac{d}{2} \omega$  for the viscosity sub-layers. This is the vorticity-transport equation, it has been shown to be a good model for topographically controlled flows, such as the one I study by Zavala and van Heijst (2002).

Recall that the relative vorticity  $\omega = \frac{\partial v}{\partial x} - \frac{\partial u}{\partial y}$ , written in form of the transport equation, is

$$\omega = \left(\frac{\psi_x}{h}\right)_x + \left(\frac{\psi_y}{h}\right)_y \quad (2.58)$$

$$\omega = \frac{\psi_{xx}}{h} - \frac{h_x \psi_x}{h^2} + \frac{\psi_{yy}}{h} - \frac{h_y \psi_y}{h^2} \quad (2.59)$$

Using scaling analysis, one can see that the terms divided by  $h^2$  are much smaller than the others. Thus, I can approximate relative vorticity as

$$\omega = \frac{\psi_{xx}}{h} + \frac{\psi_{yy}}{h} \quad (2.60)$$

In our solutions I will make the approximation that the term  $\frac{\psi_{xx}}{h}$  is dominant. I justify this approximation using scale analysis, as the cross-stream length scale is



much smaller than the streamwise. Thus, the second order derivative of  $y$  is much less important than  $x$ .

$$\omega = \frac{\psi_{xx}}{h} \quad (2.61)$$

Plugging back to equation 2.55 gives

$$\omega_t + J(\psi, q) - q(h)_t = -\frac{(f + \omega)}{h} \frac{d}{2} \omega \quad (2.62)$$

I make the final simplification by dropping the  $\omega^2$  term on the right hand side, and neglecting the time derivative terms and seeking a solution to the steady case.

$$J(\psi, q) = -\frac{fd}{2h} \omega \quad (2.63)$$

This is the form of the vorticity-transport equation I will seek solutions to.

### *Similarity Solutions*

I attempt to find solutions to the vorticity-transport equation using a similarity solution. In the process I rewrite the equation of two spatial coordinates  $f(x, y)$  as  $f(\eta(x, y))$ . The goal is to rewrite the equation of multiple variables I want to solve in terms of a single nondimensional variable. The challenge is to find the proper similarity variable  $\eta$ , such that it will reduce the complexity of the problem to a solvable one. Similarity solutions work because the flow behavior scales spatially or temporally. This means that the similarity variable relates geometric similarities of the boundaries or dynamic similarity between flow fields Granger (1995). In this work I have geometric similarity of boundaries. After finding a similarity variable that works, I perform a transformation of coordinates of the partial derivatives. Since the equations have partial derivatives of  $x$  and  $y$  I use chain rule to rewrite in terms of the similarity variable  $\eta$

$$\frac{\partial \psi(x, y)}{\partial y} = \frac{\partial \psi(\eta)}{\partial y} = \frac{\partial \psi'(\eta)}{\partial \eta} \frac{\partial \eta}{\partial y} \quad (2.64)$$

## CHAPTER THREE

### Solutions to the Model Equations

In this chapter, I will seek solutions the equations that were derived in chapter 2. I will be looking at two special cases and will expand the two dimensional interior flow solution to a three dimensional model by inclusion of the assumed Ekman layer.

#### *Expanding Jet Solution*

To model the continental slope I consider a domain where the mid-depth,  $h_o$ , is located at  $x = 0$ , the shallow side is in the positive  $x$  direction and the deep side on the negative. I define the depth with a function  $h = h_o - \alpha xy^{-\gamma}$ . Kuehl (2014) first found an analytic solution to this topography for a special case of an expanding jet of fluid, I will follow the same procedure in this section.

Earlier I derived the equations necessary for modeling the flow in a region of the ocean with a sloping bottom. The resulting equation 2.63 describes the interior flow. I need to define the boundary conditions to solve the equation and I must define the boundary conditions in terms of transport to apply them to the vorticity-transport equation.

$$\psi(\infty, y) = Q \tag{3.1}$$

$$\psi(-\infty, y) = 0 \tag{3.2}$$

$$\psi(x, 0) = Q \operatorname{erf}(x) \tag{3.3}$$

Equations 3.1 and 3.2 impose a condition that there must be a flow in the direction of  $y$  which is defined by the total transport  $Q$ . While the boundary conditions extend to infinity, this can be thought of as a long distance relative to the scale of the

problem. The boundary condition 3.3 works as a source for the flow to be initialized, while this is an unphysical condition, I can choose the proper  $y$  and  $x$  boundaries to limit ourselves to solutions of physical relevance. Figure 3.1 is a sketch of the domain I have constructed

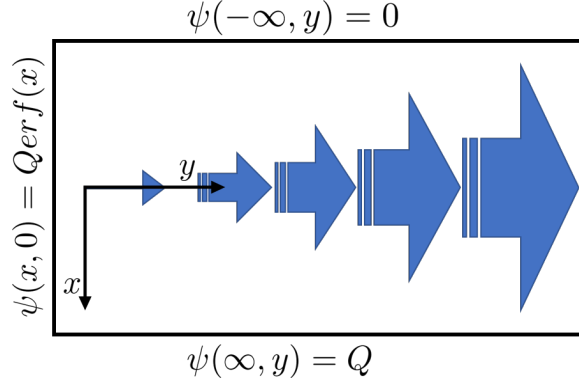


Figure 3.1: A diagram of the domain. The origin of the coordinate system, the three boundary conditions and the expected general flow field form is shown.

With the boundary conditions defined, I now turn to the vorticity-transport equation in the simplified form I derived in chapter 2.

$$J(\psi, \omega) = -\frac{df}{2} \frac{\psi_{xx}}{h^2} \quad (3.4)$$

Expanding the Jacobian gives

$$J(\psi, \omega) = -h_y \frac{f\psi_x}{h^2} - \frac{\psi_x \psi_{xxy}}{h^2} + 2h_y \frac{\psi_x \psi_{xx}}{h^3} + h_x \frac{f\psi_y}{h^2} - \frac{\psi_y \psi_{xxx}}{h^2} - 2h_x \frac{\psi_y \psi_{xx}}{h^3} \quad (3.5)$$

The terms divided by  $h^3$  will be of much smaller order than the rest, so I can drop those and obtain

$$J(\psi, \omega) = -h_y \frac{f\psi_x}{h^2} - \frac{\psi_x \psi_{xxy}}{h^2} + h_x \frac{f\psi_y}{h^2} - \frac{\psi_y \psi_{xxx}}{h^2} \quad (3.6)$$

I assume that the dominant terms in the equation are the linear ones, and that the equation to solve is

$$h_x \frac{f\psi_y}{h^2} - h_y \frac{f\psi_x}{h^2} = -\frac{df}{2} \frac{\psi_{xx}}{h^2} \quad (3.7)$$

Note that equation 3.7 is similar to that of the heat equation  $T_t = \lambda T_{xx}$ . For the special case where the equation can be reduced to equation 3.8. Previous studies have found solutions of the form  $\psi = \text{erf}(\Lambda x)$ , where  $\Lambda$  is some constant (Pijush K. Kundu, 2011). These solutions are obtained using a similarity variable approach, which encourages us to try the same.

$$h_x \frac{f\psi_y}{h^2} = -\frac{df}{2} \frac{\psi_{xx}}{h^2} \quad (3.8)$$

I use a similarity variable to transform equation 3.7 to a simpler, solvable form. The similarity variable is defined as

$$\eta = x(ky)^n \quad (3.9)$$

Where  $k$  and  $n$  are constants. Rewriting equation 3.7 using a normalized transport function

$$g(\eta) = \frac{\psi(x, y)}{Q} \quad (3.10)$$

where

$$g_x = g' \eta_x = g'(ky)^n \quad (3.11)$$

$$g_y = g' \eta_y = g' n x (ky)^{n-1} \quad (3.12)$$

$$g_{xx} = g''(ky)^{2n} \quad (3.13)$$

Where the primes indicate derivatives with respect to  $\eta$ . Substituting into equation 3.7 gives

$$-h_y \frac{fQg_x}{h^2} + h_x \frac{fQg_y}{h^2} = -\frac{d}{2} \frac{Qg_{xx}}{h^2} \quad (3.14)$$

$$h_x \frac{fQg'nx(ky)^{n-1}}{h^2} - h_y \frac{fQg'(ky)^n}{h^2} = -\frac{df}{2} \frac{Qg''(ky)^2}{h^2} \quad (3.15)$$

Substituting  $h = h_o - \alpha xy^{-\gamma}$  and analyzing, I find solutions to the differential equation under the following conditions

$$n = -\frac{1+\gamma}{2} \quad (3.16)$$

$$k = \left(\frac{\alpha}{2d}\right)^{\frac{1}{2n}} \quad (3.17)$$

$$-1 \leq \gamma < 1 \quad (3.18)$$

The solution takes the form of

$$\psi = Q\left[\frac{erf(\eta) + 1}{2}\right] \quad (3.19)$$

In Kuehl (2014) it was found that the value of  $\gamma$  is related to the shape of the flow.  $\gamma > -1$  results in an expanding flow to of the solution. For  $\gamma \leq -1$  the increased slope would produce a compressing jet. In the next section I present my approach for the compressing jet case.

### *Compressing Jet Solution*

In the previous section I presented an analytic solution for an expanding jet of fluid over a sloping topography. In this section, I present d a solution for the compressing jet case. The domain is essentially the same, but condition 3.3 changes to

$$\psi(x, \infty) = Qerf(x) \quad (3.20)$$

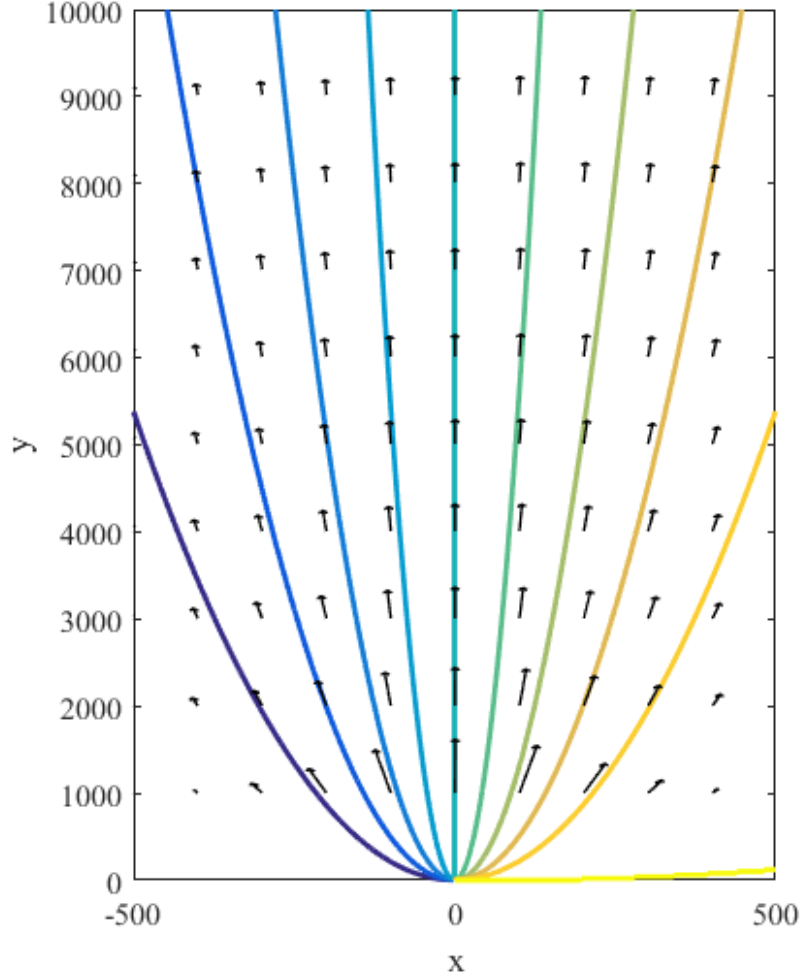


Figure 3.2: Plot of the velocity field and the transport. The contour lines represent transport isolines. The velocity field is normalized by the maximum velocity.

Note that in this case the boundary conditions is a sink instead of a source. This means that the solution will have to converge towards a singularity downstream. Like in the previous case, I also distance myself from the limits of the domain, as they lose physical significance. Figure 3.3 shows a sketch of the domain.

Additionally, I know from Kuehl's study that I will be looking for a topography of the form  $h = h_o - \alpha xy^{-\gamma}$  where  $\gamma < -1$ . Now I go back to the vorticity-transport equation but retain the nonlinear terms.

$$-h_y \frac{f\psi_x}{h^2} - \frac{\psi_x \psi_{xxy}}{h^2} + h_x \frac{f\psi_y}{h^2} - \frac{\psi_y \psi_{xxx}}{h^2} = -\frac{fd}{2} \frac{\psi_{xx}}{h^2} \quad (3.21)$$

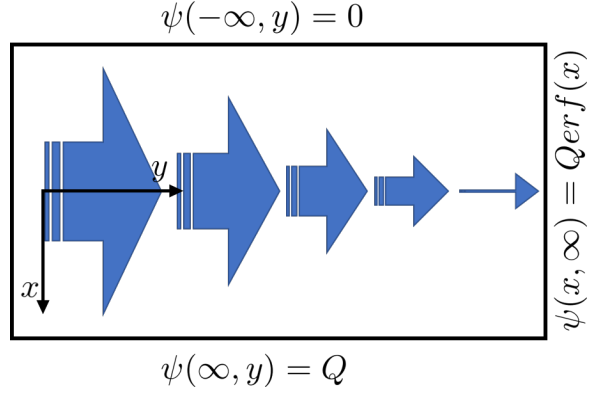


Figure 3.3: Sketch of the domain.  $U$  is the stream velocity scale,  $\Omega$  is the frame rotation scale,  $h_o$  is the depth scale and  $L$  is the plane length scale.

In this analysis I use a similarity variable of the form

$$\eta = Cx^ay^b \quad (3.22)$$

Where  $a$ ,  $b$  and  $C$  are constants. Like in the previous solution, I define a normalized transport function  $g(\eta) = \psi(x, y)/Q$  and substitute it into equation 3.21

$$-h_y f g_x - g_x g_{xxy} + h_x f g_y - g_y g_{xxx} = -\frac{fd}{2} g_{xx} \quad (3.23)$$

Then I perform the same operations as with the previous solution. Expanding the derivative terms gives

$$g_x = aCx^{a-1}y^bg' \quad (3.24)$$

$$g_y = bCx^ay^{b-1}g' \quad (3.25)$$

$$g_{xx} = a^2C^2x^{2(a-1)}y^{2b}g'' + a(a-1)Cx^{a-2}y^bg' \quad (3.26)$$

$$\begin{aligned} g_{xxx} = & (a^3C^3x^{3(a-1)}y^{3b})g''' + \\ & 3g''(aCx^{a-1}y^b)(a(a-1)Cx^{a-2}y^b) \\ & + g'(a(a-1)(a-2)Cx^{a-3}y^b) \end{aligned} \quad (3.27)$$



$$\begin{aligned}
g_{xy} &= g'''(a^3 C^3 x^{3(a-1)} y^{3b}) \\
&+ 3g''(\eta)(a C x^{a-1} y^b)(a(a-1) C x^{a-2} y^b) \\
&+ g'(\eta)(a(a-1)(a-2) C x^{a-3} y^b)
\end{aligned} \tag{3.28}$$

Substitute these equations into equation 3.23

$$\begin{aligned}
&h_x/Q(fg' C x^a b y^{b-1}) - h_y/Q(fg' C a x^{a-1} y^b) \\
&+ Q^{-2}((g')^2 C^2 a^2 (a-1) x^{2a-3} b y^{2b-1} \\
&- (g')^2 C^2 a (a-1)(a-2) x^{2a-3} b y^{2b} \\
&+ g' g'' C^3 a^3 x^{3a-3} b y^{3b-1} \\
&- g' g'' C^3 a^2 (a-1) x^{3a-3} b y^{2b} ((a-1)x^{-1} + 2y^{b-1}) \\
&+ g' g''' C^4 a^3 x^{4a-4} b y^{4b-1} - g' g''' C^4 a^3 x^{4a-4} b y^{4b-1}) \\
&= -fd/2[g' C a (a-1) x^{a-2} y^b + g''(C a x^{a-1} y^b)^2]
\end{aligned} \tag{3.29}$$

The terms of  $g' g'''$  cancel, leaving only the terms of  $(g')^2$  and  $g' g''$  for the non-linear part. If I let  $a = 1$  the terms of  $(g')^2$  become zero. This assumption is related to linear sloping of the topography in  $x$ .

$$h_x f g' x b y^{b-1} - h_y f g' y^b + 2Q g' g'' b y^{3b-1} = -fd/2 g'' y^{2b} \tag{3.30}$$

The equation is greatly reduced, and if I let  $b = 1$  it further simplifies to

$$h_x f g' x y^{-2} - h_y f g' y^{-1} + 2Q g' g'' = -fd/2 g'' \tag{3.31}$$

By inspection I note that if I introduce a topography of the form  $h = h_o - \alpha x y^3$ , which also satisfies the condition of  $\gamma < -1$ , I am able to eliminate all variables  $x$  and  $y$ , and obtain a differential equation in terms of  $\eta$

$$\frac{4\alpha}{dC^2} \eta g' + g'' + \frac{2QC}{fd} g' g'' = 0 \tag{3.32}$$

I rearrange and define the constants  $A = \frac{dC^2}{4\alpha}$  and  $B = \frac{QC^3}{2f\alpha}$  for easier manipulation, which results in

$$\eta g' + Ag'' + Bg'g'' = 0 \quad (3.33)$$

It is then clear that  $B$  scales the nonlinear component, while  $A$  the linear. I solve equation 3.33 by using substitution and separation of variables. I define a substitution variable  $\kappa = g'$  and manipulate

$$\eta\kappa + A\kappa' + B\kappa\kappa' = 0 \quad (3.34)$$

$$\eta\kappa + A\frac{d\kappa}{d\eta} + B\kappa\frac{d\kappa}{d\eta} = 0 \quad (3.35)$$

$$(A + B\kappa)d\kappa = -(\eta\kappa)d\eta \quad (3.36)$$

$$\frac{A + B\kappa}{\kappa}d\kappa = -(\eta)d\eta \quad (3.37)$$

Integrating both sides gives

$$-(B\kappa + A\ln[\kappa]) = \frac{\eta^2}{2} + m \quad (3.38)$$

where  $m$  is a constant of integration. It is possible to solve for  $\kappa$  using a special function  $W(\eta)$  called the Lambert-W function, see appendix A for more detail about the Lambert-W function. Solving for  $\kappa$  gives

$$\kappa = \frac{A W\left(\frac{B}{A}e^{-\frac{2m+\eta^2}{2A}}\right)}{B} \quad (3.39)$$

Recall that  $\kappa = g'$  is a sudo velocity, so to obtain the transport equation I must integrate equation 3.39. Since this equation cannot be integrated analytically, I limit myself to the linear case  $B = 0$ . To study this case I take the limit of equation 3.39 as  $B$  goes to 0

$$\lim_{B \rightarrow 0} g' = e^{-\frac{2m+\eta^2}{2A}} \quad (3.40)$$

Integrating gives us the transport function for the linear equation

$$g = \sqrt{\frac{A\pi}{2}} e^{-\frac{m}{A}} \operatorname{erf}\left(\frac{\eta}{\sqrt{2A}}\right) + n \quad (3.41)$$

where  $n$  is some constant of integration. Applying the boundary conditions 3.1 and 3.2 to 3.41 tells us that  $n = \frac{1}{2}$  and  $m = A \ln(\sqrt{2A\pi})$  giving the transport equation

$$g = \frac{1}{2} \operatorname{erf}\left(\frac{\eta}{\sqrt{2A}}\right) + \frac{1}{2} \quad (3.42)$$

This linear solution has the same form to that of the expanding jet case when  $A = \frac{1}{2}$ , but this solution is for a different set of conditions. Thus, I have successfully expanded the set of cases one can study using analytic methods.

Now, let us examine the case where the nonlinear term  $B$  is retained. Equation 3.39 cannot be integrated with an analytic method, but I need to obtain the transport in order to apply the boundary conditions to find  $m$ . I use numerical methods solve this part of the problem. The first thing to note is that the boundary conditions are defined at infinite distances, this is accounted for in the numerical approach by using a large domain in the process, which works as an approximation to infinite conditions. First, I integrate equation 3.39 using a trapezoidal method and with an initial guess for  $m$ . The boundary condition 3.1 is met (this means the added integration constant is equal to 0), but the boundary condition 3.2 is dependent on the value of  $m$ . To find  $m$  I use an iterating scheme that searches for the appropriate value of  $m$  so that all boundary conditions are met. Once I find  $m$ , the problem is completely solved. I can now describe the interior flow, while keeping the nonlinear effects.

To confirm the validity of the approach, I numerically solve the nonlinear case using the MATLAB `bvp solve` function and a shooting forward Euler method. I find good agreement for small ratios of  $\frac{B}{A} < 0.1$ . For higher ratios, the methods became unstable, but the analytic approach is still solvable using the method I described for any value of  $\frac{B}{A}$ .

While the transport equation does not have a full analytic solution, I find that the velocity field can be described in an analytic form.

$$\psi_x = hv = Q \frac{dg}{d\eta} \frac{d\eta}{dx} \quad (3.43)$$

$$\psi_y = -hu = Q \frac{dg}{d\eta} \frac{d\eta}{dy} \quad (3.44)$$

converting the similarity variable back to  $x$  and  $y$  coordinates gives

$$v = Q \frac{g' C y}{h} \quad (3.45)$$

$$u = -Q \frac{g' C x}{h} \quad (3.46)$$

I compare the nonlinear solution to the linear to check that the numerical method converges to the linear case as I decrease  $B$ . Figure 3.4 shows a comparison of different ratios of  $\frac{B}{A}$  and the linear case. This comparison also demonstrates the effects of the nonlinear terms in the dynamics. As the nonlinear term becomes bigger, the width of the jet slowly increases. This is related to the inertial term in the equations of motion.

So far I have ignored the constant  $C$  in the similarity variable. This constant is related to the rate of contraction of the flow field and scales the linear and nonlinear component. If  $C > 1$  then the nonlinear term is scaled up, and the linear down and if  $C < 1$  the opposite happens. When plotting the linear solution and the nonlinear solution, one can see that the effect of the nonlinear component is to slow down the rate of contraction of the jet, as seen in figure 3.5.

### *Extension of Solutions*

I can extend both solutions to describe the flow field from the bottom boundary to the interior flow by using the Ekman layer solutions. Recall that equations 2.39 and 2.40 need the interior flow velocities to be solved. So, the solutions found in section

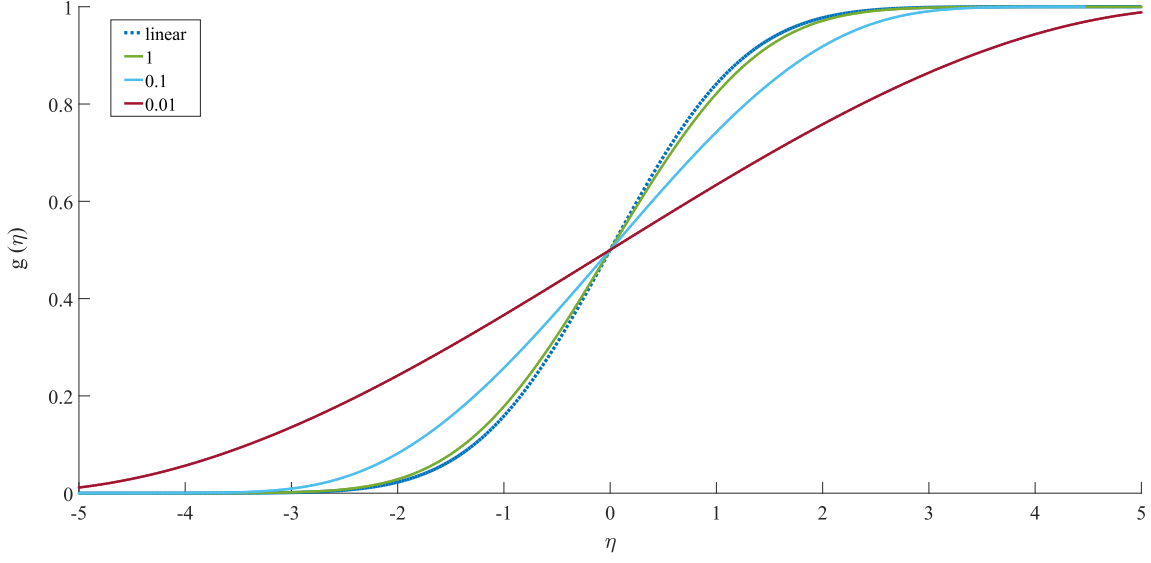


Figure 3.4: A plot of the normalized transport solution in similarity variable space. There are four lines plotted. One is the linear solution ( $B = 0$ ) and the other three have the value of  $B/A$  in the legend, where  $A = 1$ .

3.1 and 3.2 give the values of  $\bar{u}$  and  $\bar{v}$ . Then by plugging in these values to equations 2.39 and 2.40, a flow field that takes into account the Ekman layer effects is obtained.

The vertical velocity  $w$  can be determined by integrating the following equation

$$\begin{aligned} \frac{\partial w}{\partial z} = & e^{\left(\frac{b-z}{d}\right)} \left[ \left( \frac{\partial \bar{v}}{\partial x} - \frac{\partial \bar{u}}{\partial y} \right) \sin\left(\frac{z-b}{d}\right) \right. \\ & + \frac{1}{d} \frac{\partial b}{\partial x} ([\bar{u} - \bar{v}] \cos\left(\frac{z-b}{d}\right) + [\bar{u} + \bar{v}] \sin\left(\frac{z-b}{d}\right)) \\ & \left. + \frac{1}{d} \frac{\partial b}{\partial y} ([\bar{u} + \bar{v}] \cos\left(\frac{z-b}{d}\right) + [\bar{u} - \bar{v}] \sin\left(\frac{z-b}{d}\right)) \right] \end{aligned} \quad (3.47)$$

Since  $\bar{u}$  and  $\bar{v}$  are independent of  $z$  integrating gives

$$w = e^{\frac{b-z}{d}} \left( -\left[ \frac{\partial b}{\partial x} (\bar{u} - \bar{v}) + d \left( \frac{\partial \bar{v}}{\partial x} - \frac{\partial \bar{u}}{\partial y} \right) \cos\left(\frac{z-b}{d}\right) - \left( \frac{\partial b}{\partial x} + \frac{\partial b}{\partial y} \right) (\bar{u} + \bar{v}) \sin\left(\frac{z-b}{d}\right) \right] \right) \quad (3.48)$$

Note from equations

$$\psi_x = hv \quad (3.49)$$

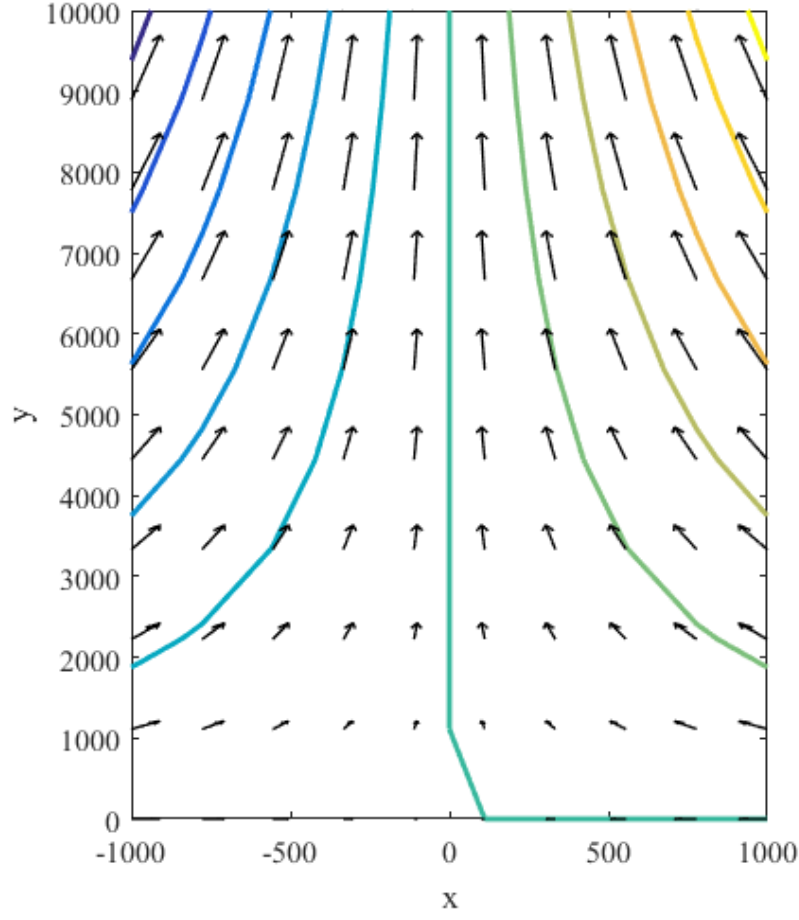


Figure 3.5: Plot of the velocity field and the transport. The contour lines represent transport isolines. The velocity field is normalized by the maximum velocity

$$\frac{\partial \bar{v}}{\partial x} = \frac{\partial}{\partial x} \left( \frac{\psi_x}{h} \right) = \frac{\psi_{xx}}{h} - h_x \frac{\psi_x}{h^2} \quad (3.50)$$

which in terms of the normalized transport equation using the similarity variable is

$$\frac{\partial \bar{v}}{\partial x} = \frac{\psi_{xx}}{h} - h_x \frac{\psi_x}{h^2} = \frac{Qa^2C^2y^2g''}{h} - h_x \frac{QCyg'}{h^2} \quad (3.51)$$

and for  $\bar{u}$

$$-\frac{\partial \bar{u}}{\partial y} = -\frac{\partial}{\partial y} \left( \frac{\psi_y}{h} \right) = \frac{\psi_{yy}}{h} - h_y \frac{\psi_y}{h^2} \quad (3.52)$$

Which can also be solved using the solutions I found. At this point all that is needed is to plug in the values from the solution. Thus, I have created a three dimensional

model that accounts for all dominant forces with the effects introduced by viscosity through the Ekman layer.

## CHAPTER FOUR

### Applications

In this chapter I use bathymetry data from the National Oceanic and Atmospheric Administration (NOAA) ETOPO1 database to estimate flow fields in portions of the continental slope using a code I developed in MATLAB. I analyze large sections of the ocean and use the MATLAB code to determine regions where the analytic solutions are applicable. In other words, I search for regions that satisfy the topographic constraints (can be described using a topographic function  $h = h_o - \alpha xy^{-\gamma}$ ). I will present two cases, one for the sections of the continental slope along the Florida coast and a region of strong sloping near the Norwegian coast.

#### *MATLAB Code*

To start the analysis, I download topographic data from the NOAA ETOPO1 database. The data file is in the form of an .xyz file which contains coordinates and depth. The data samples I analyze are typically larger than 300 km by 300 km, because of this the raw data file is too big and impossible to process due to memory constraints. In order to convert the data size into something manageable, the code reduces the resolution of the topography by reading a limited number of grid points. This results in loss of some of the finer features of the topography, but retain the large scale shape of the slope which is what I am interested in. With the reduced data, the code applies a thin-plate interpolation surface fit. This generates a single continuous function that can give the depth at any point in  $x$  and  $y$ , with this function it becomes much easier to process and search for regions of interest.

Now that the data is easy to process, I manually input the middle depth  $h_o$  of the region of interest. The code identifies the points that define the isobath line



for  $h_o$ . From the physics of the flow, I expect the mean flow to approximately follow isobath lines due to conservation of potential vorticity. Because the flow follows the isobath I can define the origin of the  $x$  axis ( $x = 0$ ) to be located at  $h_o$ . Thus the coordinate system is defined such that the  $h_o$  isobath is the streamwise direction and orthogonal lines are the cross-stream distance.

The code calculates the points that define orthogonal lines to the isobath to find the local slope in the  $x$  direction. The orthogonal lines have a length which is manually inputted to ensure they capture the entire continental slope region. In other words, the orthogonal lines will extend from the continental shelf to the basin. Inserting the  $x$  and  $y$  points that define the orthogonal lines into the surface fit I generated earlier gives the depth  $h$  at each point of the orthogonal line. Then the code applies a linear fit of the form  $h(x) = \alpha_x x + \beta$  of  $h$  versus  $x$  at each orthogonal line. This line fit gives the local slope in the  $x$  direction  $\alpha_x$ , note that  $\beta$  has to be  $h_o$  because I have defined  $h(0) = h_o$ . The code has defined  $\alpha_x$  and can relate it to a position in  $y$  by calculating the distance between each orthogonal line center. Then the code fits curves to  $\alpha_x$  versus  $y$  which give the change of the slope in  $x$  in the streamwise direction, i.e. as a function of  $y$ . The curves fitted to  $\alpha_x$  versus  $y$  are of the form  $\alpha_x(y) = \alpha_y(y - y_o)^{-\gamma}$ , where  $y_o$  is a shift in the  $y$  direction and  $\gamma$  is the constant related to the topographic constraint of the analytic solutions. If the code finds a good fit for a value of  $\gamma$  and satisfies the topographic constraints, then it has found a section of the ocean in the data set where the flow field can be calculated using the analytic solutions.

To obtain the topographic function from the fitted function, to the form  $h(x, y) = \alpha_x y^{-\gamma} - h_o$  as defined in the analytic solutions, I need to use the fit parameters  $\alpha_x$  and  $y_o$ . Recall that the first fitted line defines  $h(x) = \alpha_x x - h_o$  at a specific point in  $y$ . The code also determined a curve that defines  $\alpha_x$  as a function of  $y$ . So, by combining both functions I can write  $h(x, y) = \alpha_y(y - y_o)^{-\gamma} x - h_o$ , which with the appropriate selection of  $y$  it can be rewritten as  $h(x, y) = \alpha_y y^{-\gamma} x - h_o$ , thus  $\alpha_y = \alpha$ .

The appropriate selection of  $y$  is a shift in the coordinate, so  $y^* = y - y_o$ , where  $y^*$  is the appropriate downstream coordinate.

The code is available for download online at [www.ruyibanez.com](http://www.ruyibanez.com) .

### *Examples*

From the examples I present, it will be clear that there are many cases in the ocean where the topography is approximately  $h = h_o - \alpha xy$ , ( $\gamma = -1$ ). For the contracting solution if  $\alpha$  is very small it will result in nearly uniform flow fields, as a consequence the flow fields may not appear contracting or expanding to the eye in the examples, since the effects are very subtle. And for  $\gamma = 1$  in the expanding jet solution it results in a uniform flow. The Ekman effects are captured in the flow field and is shown by the spiraling of the velocity in near the bottom.

### *Gulf of Mexico*

Applying the MATLAB code to a section of the continental slope region off the Florida coast. The analyzed region is located at  $86.2^\circ$  west,  $82.9^\circ$  west,  $29.7^\circ$  north and  $23.9^\circ$  north and I choose the middle depth to be  $h_o = 1250$  m. Figure 4.1 shows the points that are sampled to determine  $\alpha_x$

Figure 4.2 shows the  $\alpha_x$  versus  $y$  plot. It shows multiple regions where a solution can be applied. I present the solution for the region with the slope  $\alpha = 1.5 \cdot 10^{-6} \text{ m}^{-1}$ . I apply the expanding jet solution with the Ekman layer expansion. The parameters I use are the following

$$x = -7.5 \text{ km to } 7.5 \text{ km}$$

$$y = 21 \text{ km to } 63 \text{ km}$$

$$h_o = 1250 \text{ m}$$

$$\nu_E = 10^{-2} \text{ m}^2/\text{s}$$

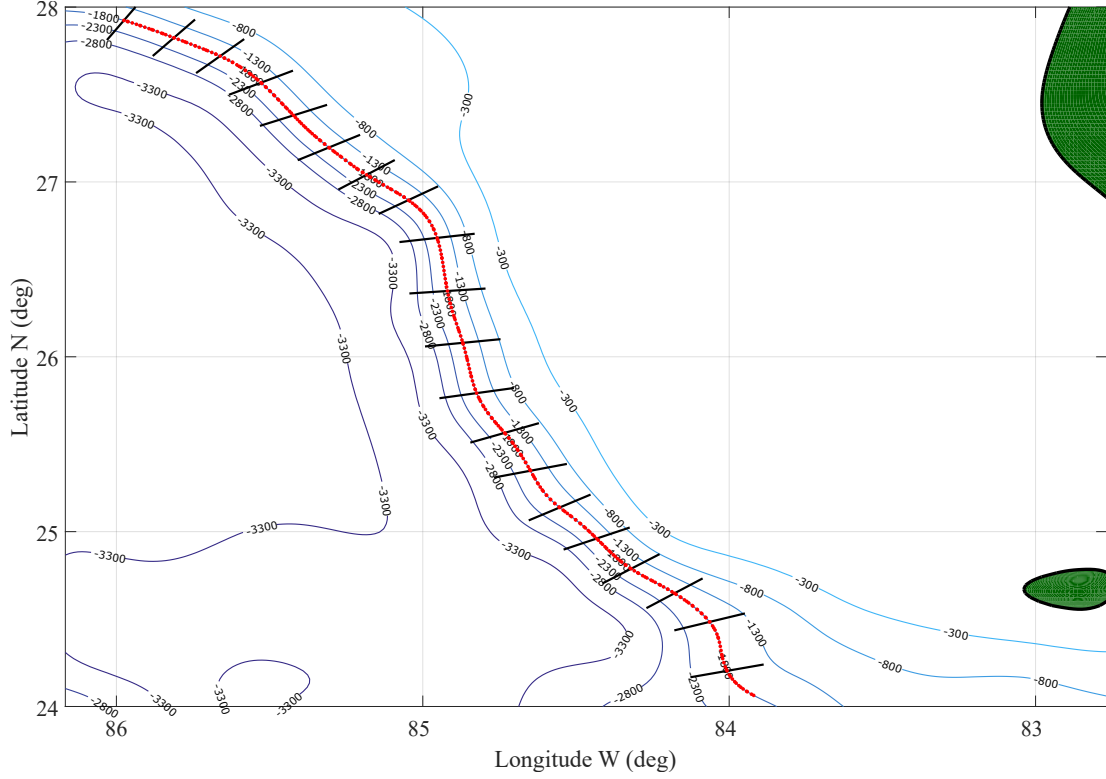


Figure 4.1: Shown is a map of the region of interest near the Florida coast. The red dots symbolize the locations that are sampled for orthogonal  $\alpha_x$  fits. The length of the sample is shown in some cases as the black orthogonal lines.

$$Q = 10^6 \text{ m}^2/\text{s}$$

The resulting velocity field is plotted in figure 4.3.

### *Norwegian Coast*

I look at a sloping region by the Norwegian coast located at  $3.6^\circ$  east,  $12.4^\circ$  east,  $64.6^\circ$  north and  $68.5^\circ$  north. I perform the same procedure as with the Florida coast. For brevity I will only show the equivalent figures to the previous analysis.

The parameters I use are the following

$$x = -10 \text{ km to } 10 \text{ km}$$

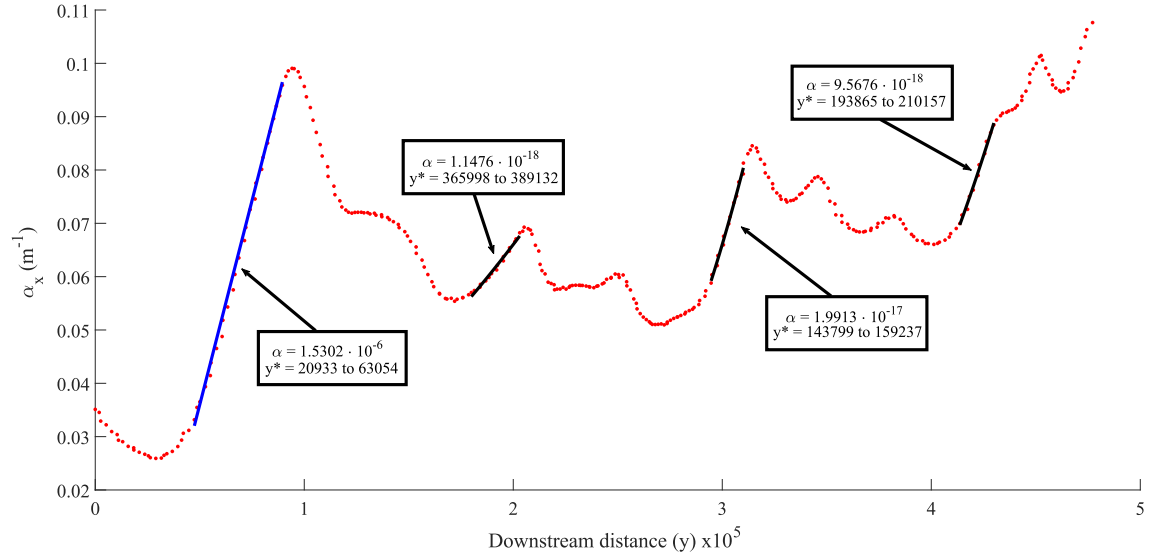


Figure 4.2: The blue line is a linear fit, so it shows a region that can be described as  $h = h_o - \alpha xy$ . The black line is a cubic fit, which means it the region can be described as  $h = h_o - \alpha xy^3$ . The labels indicate the value of  $\alpha$  and the range of  $y^*$  for each fit

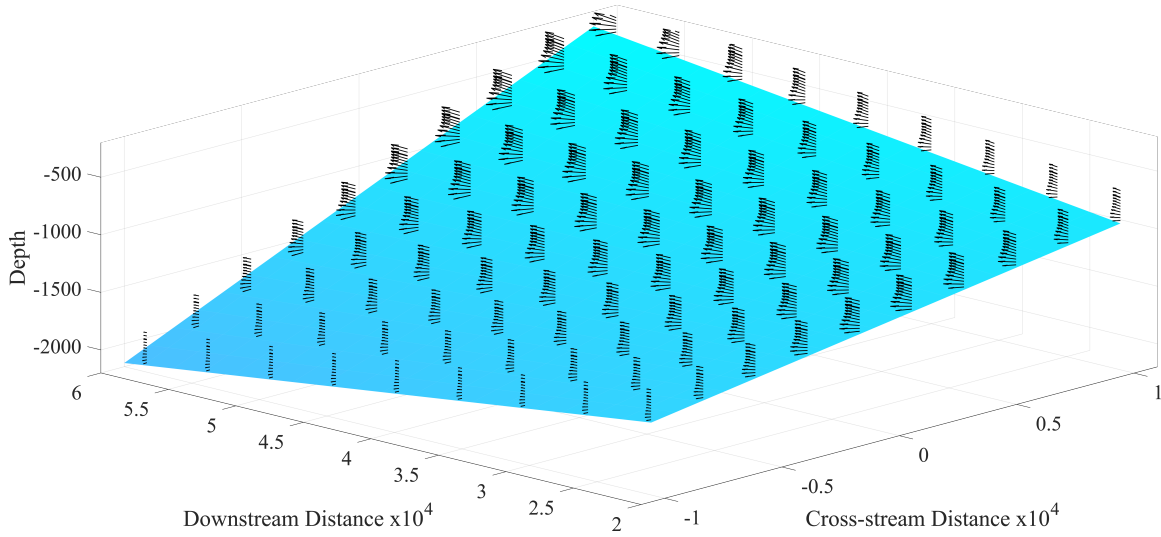


Figure 4.3: Resulting velocity field and topography for the region of interest in the Florida coast. All axis are in meters.

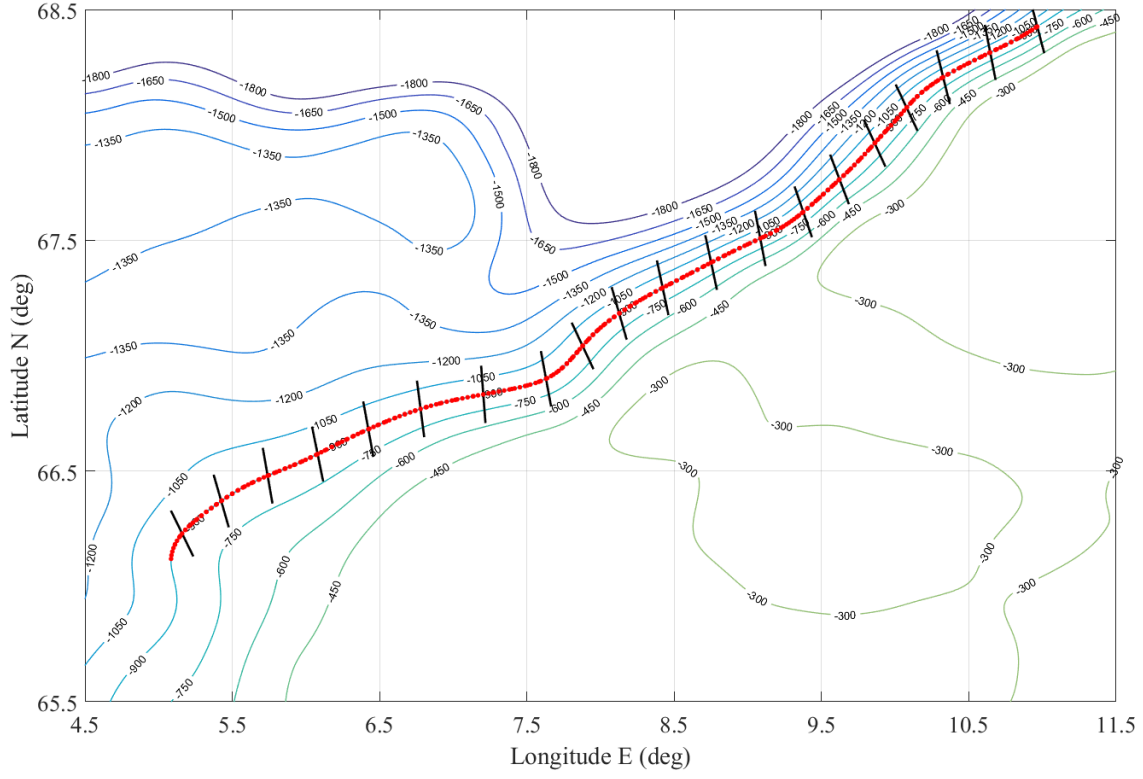


Figure 4.4: Shown is a map of the region of interest near the Florida coast. The red dots symbolize the locations that are sampled for orthogonal  $\alpha_x$  fits. The length of the sample is shown in some cases as the black orthogonal lines.

$$y = 385 \text{ km to } 400 \text{ km}$$

$$h_o = 900 \text{ m}$$

$$\nu_E = 10^{-2} \text{ m/s}^2$$

$$C = 10^{-2} \text{ m}^{-2}$$

$$Q = 10^7 \text{ m}^2/\text{s}$$

$$\alpha = 6.3 \cdot 10^{-19} \text{ m}^{-3}$$

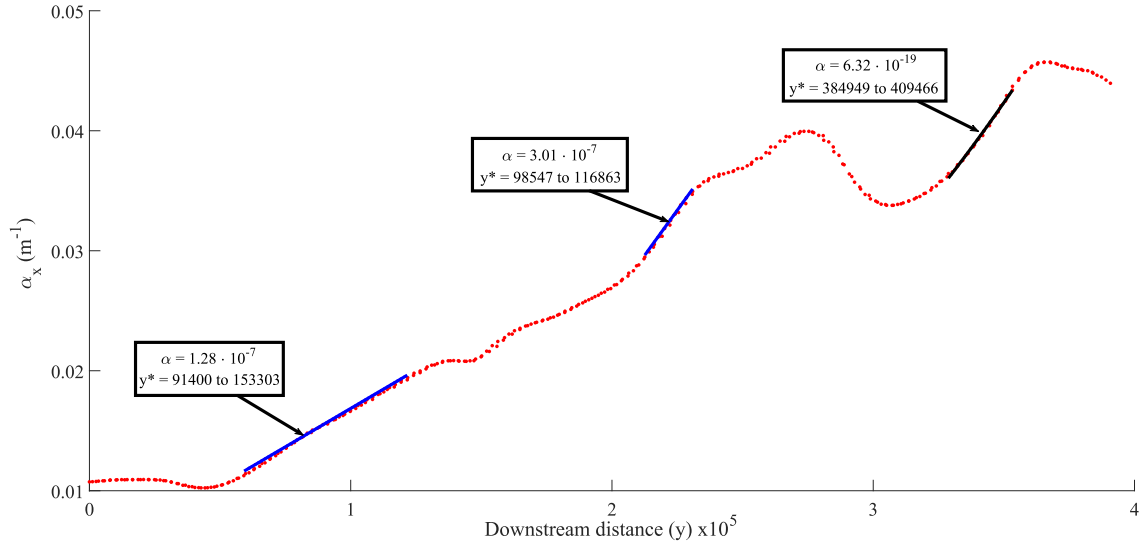


Figure 4.5: The blue line is a linear fit, so it shows a region that can be described as  $h = h_o - \alpha xy$ . The black line is a cubic fit, which means it the region can be described as  $h = h_o - \alpha xy^3$ . The labels indicate the value of  $\alpha$  and the range of  $y^*$  for each fit

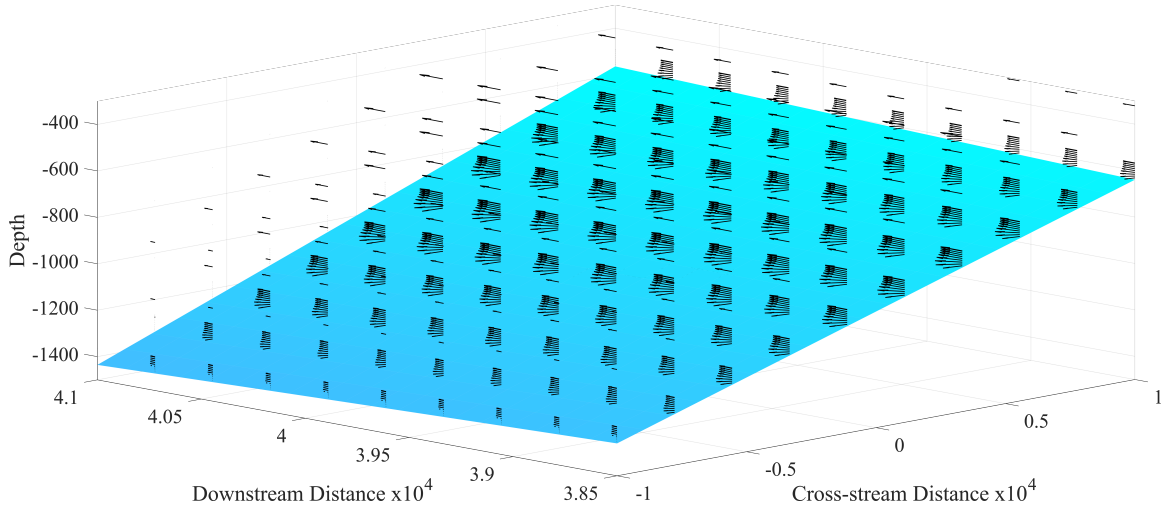


Figure 4.6: Resulting velocity field and topography for the region of interest in the Norwegian coast. All axis are in meters.

## CHAPTER FIVE

### Conclusion

#### *Summary*

I have found an analytic solutions using similarity variables for flow fields with sloping sections in the ocean. I constructed the model by determining the dominant dynamics using scaling arguments, thus simplifying the equations of motion so that I am able to obtain solutions of the base flow in special cases. These special cases are related to the topographic geometry and I proved in the applications section that these geometries can be commonly found in regions of the ocean. The compressing jet solution provides insight into the effects of the nonlinear inertial terms in the equations. I find that the inertia tends to resist a change in the flow field. The effects may or may not be of relevance depending on the parameters of the specific domain, which means that for slower flows the linear solution can be a good approximation. This solution shows the consistency of using the methods Kuehl (2014) used for the expanding jet. It is possible that by modifying the similarity variable I can find solutions to other special cases. Finally, I expanded the two dimensional solutions into a three dimensional base flow solution that accounts for the low order viscous effects.

#### *Future Work*

While the analytic solution shows properties that are consistent with the properties of geophysical flows in the ocean, I cannot guarantee that the approximation is accurate until I have observational and/or experimental data. At the time of writing, I am building a rotating tank experiment which will be able to replicate the conditions I studied in this analytic work.

In the introduction I emphasized the importance of the understanding the mechanisms of transport in the ocean. One of the benefits that the analytic solutions provide, are that one can use Lagrangian methods to find analytic characteristics of transport. I have performed preliminary calculations using lobe dynamics as in Samelson and Wiggins (2000) and found that the implementation of the Ekman effects into the flow solutions generate mixing regions along the  $h_o$  isobath, which can be a mechanism of transport between the shallow and deep side of the topography. This needs to be studied further, it could be an important result, as these topographic conditions are typically considered barriers of transport to the dynamics of potential vorticity.



## APPENDICES

## APPENDIX A

### Lambert W function

Following Corless, Gonnet, Hare, Jeffrey, and Knuth (1996), the Lambert W function, also known as the product log, is the inverse function

$$f^{-1}(xe^x) = W(x) \quad (\text{A.1})$$

The function is described by an infinite series

$$W(x) = \sum_{k=1}^{\infty} \frac{(-k)^{k-1} x^k}{k!} \quad (\text{A.2})$$

In our solution we require to solve an equation of the following form

$$a \ln(x) + bx = -\frac{y^2 + c}{2} \quad (\text{A.3})$$

if we exponentiate both sides

$$x^a e^{bx} = e^{-\frac{y^2 + c}{2}} \quad (\text{A.4})$$

Now take the power of  $\frac{1}{a}$  of both sides

$$xe^{\frac{b}{a}x} = e^{-\frac{y^2 + c}{2a}} \quad (\text{A.5})$$

Multiplying by  $\frac{b}{a}$  on both sides allows us to use the W Lambert definition

$$\frac{b}{a} x e^{\frac{b}{a}x} = \frac{b}{a} e^{-\frac{y^2 + c}{2a}} \quad (\text{A.6})$$

Which using the definition gives

$$\frac{b}{a} x = W\left(\frac{b}{a} e^{-\frac{y^2 + c}{2a}}\right) \quad (\text{A.7})$$

## APPENDIX B

### Matlab Code

#### *Contents*

- Define h<sub>o</sub>
- depth Adjustment (for lakes)
- Plotting range
- Data reader
- Conversion
- centering x and normalzing everything
- Fitting thinplateinterp
- Scaling operation for roatation this function has been removed, it is redundant.
- Normalized plot of region

```
clc
```

```
clear all
```

```
close all
```

```
Define ho
```

```
follow = 1800;
```

```
% follow = 900;
```

```
% follow = 100;
```

```
depth Adjustment (for lakes)
```

```
zadj = 0;
```

```
% zadj = 183; % Coast line height
```

*Plotting range*

```
clines = -20:-15:-500;

clines = -300:-500:-4000;
% clines = -300:-150:-1800;
```

*Data reader*

```
reading xyz file

fileID = uigetfile('.../*.xyz');
file_name = fileID;
xyzreader(fileID) % This function just reads an xyz file and converts it to something
load('A')

x = double(A(:,1));
y = double(A(:,2));
z = double(A(:,3))-zadj;

% center coordinates of section
thetaavg = mean([max(x) min(x)]);
phiavg = mean([max(y) min(y)]);

disp('coordinates x:')
West = min(x)
East = max(x)

disp('coordinates y:')
South = min(y)
North = max(y)
```

### *Conversion*

x-length y-length Convert to cartesian

```
theta_1 = min(x);
```

```
theta_2 = max(x);
```

```
phi_1 = 90-min(y);
```

```
phi_2 = 90-max(y);
```

```
Earth_radius = 6367;
```

```
theta_delta = abs(max(x)-min(x));
```

```
phi_delta = abs(max(y)-min(y));
```

```
x_length = [Earth_radius*cosd(theta_1)*sind(phi_1) Earth_radius*cosd(theta_2)*sind(phi_2)];
```

```
y_length = [Earth_radius*sind(theta_1)*sind(phi_1) Earth_radius*sind(theta_2)*sind(phi_2)];
```

```
z_length = [Earth_radius*cosd(phi_1) Earth_radius*cosd(phi_2) Earth_radius*cosd(phi_3)];
```

```
for i = 1:4
```

```
    R_vector(i,:) = [x_length(i),y_length(i),z_length(i)];
```

```
end
```

```
% As a note: 1-NW 2-NE 3-SW 4-SE
```

```
Sx = norm(R_vector(2,:)-R_vector(4,:))
```

```
Sy = norm(R_vector(1,:)-R_vector(2,:))
```

```
centering x and normalizing everything
```

```
x = x - min(x);
```

```
x = x/max(x);
```

```
x = x - max(x)/2;
```

```
y = y - min(y);
```

```
y = y/max(y);
```

```
y = y - max(y)/2;
```

*Fitting thinplateinterp*

```
A = [x y z]*rotz(0);
```

```
x = (A(:,1));
```

```
y = (A(:,2));
```

```
z = (A(:,3));
```

```
T = table(x,y,z);
```

```
f = fit([T.x, T.y],T.z,'thinplateinterp');
```

*Scaling operation for roatation this function has been removed, it is redundant.*

```
Rx = [-Sx/2 -Sx/2 Sx/2 Sx/2];
```

```
Ry = [-Sy/2 Sy/2 -Sy/2 Sy/2];
```

```
Rz = [1 1 1 1];
```

```
SRA = [Rx' Ry' Rz'];
```

```
% x and y scales in kilometers
```

```
Sx = abs(SRA(1,1))+abs(SRA(2,1));
```

```
Sy = abs(SRA(1,2))+abs(SRA(2,2));
```

```
lx = linspace(-0.5,0.5,250);
```

```
ly = linspace(-0.5,0.5,250);
```

```
%
```

```
X = meshgrid(lx,lx);
```

```
Y = meshgrid(ly,ly)';
```

```
Z = f(X,Y);
```

*Normalized plot of region*

```
figure(1)
```

```
hold on
```

```
view(2)
```

```
contour(X,Y,Z,clines,'ShowText','on','linewidth',1);
```

```
SSplot = contour(X,Y,Z,[-follow -follow],'ShowText','on','linewidth',3);
```

```
xlabel('x')
```

```
ylabel('y')
```

APPENDIX C

MATLAB - .xyz Reader

```
function xyzreader(fileID)
    fileID = fopen(fileID);
    C = textscan(fileID,'%f32 %f32 %f32');
    A = cell2mat(C);
    A = A(1:round(length(A))*0.001:round(length(A)),:);
    size(A)
    save('A')
    fclose('all');
end
```

Not enough input arguments.

Error in xyzreader (line 2)

```
    fileID = fopen(fileID);
```



## APPENDIX D

### MATLAB - Orthogonal Line Procedure

#### *Contents*

- Orthogonal lines
- Traveled
- Fitting
- Plot orthogonal lines
- Plot Center Points
- Flip to fit

#### *Orthogonal lines*

```
l = .05;

% StartT = round(.025*length(SSplot));
% EndT = round(.7*length(SSplot));
StartT = round(.05*length(SSplot));
EndT = round(.95*length(SSplot));

Ref = 1;

for i = StartT:round(.0025*length(SSplot)):EndT
```

```

    Before = SSplot(:,i-1);
    Center(:,Ref) = SSplot(:,i);
    After = SSplot(:,i+1);
    Tang = After-Before;
    Orth = null(Tang');
    Orthv(:, :, Ref) = Orth*linspace(-1/2,1/2,100)+Center(:,Ref);
    Orthz(:,Ref) = f(Orthv(1, :, Ref), Orthv(2, :, Ref));
    CrossL(Ref) = sqrt((Sx*1000)^2*(Orthv(1,100,Ref)-Orthv(1,1,Ref))^2+(Sy*1000)^2*(O
    Ref = Ref+1;

end

Traveled
Traveled(1) = 0;

for i = 2:length(Center)

    Moved = (Center(:,i)-Center(:,i-1));
    Moved = norm([Moved(1)*Sx*1000 Moved(2)*Sy*1000]);
    Traveled(i) = Moved+Traveled(i-1);

end

Fitting
for i = 1:length(Center)

    LLC = linspace(-CrossL(i)/2,CrossL(i)/2);
    ZZC = Orthz(:,i);
    [zlfrit,zlfitp] = fit(LLC',ZZC,'poly1');

```

```

    rsqx(i) = zlfity.rsquare;
    alphax(i)=zlfity.p1;

end

Plot orthogonal lines

figure(1)
for i = 1:length(Center)
    hold on
    plot(Orthv(1,:,i),Orthv(2,:,i),'k-')
end

Plot Center Points

figure(1)
hold on
plot(Center(1,:),Center(2,:), 'r.', 'markersize',12)
plot(Center(1,1),Center(2,1), 'b.', 'markersize',18)

Flip to fit

flipper = input('flip? yes = 1 no = 0: ');

if flipper == 0
    figure(9)
    hold on
    plot(Traveled,alphax,'r-','linewidth',1.5)
    % plot(alpha,'r-','linewidth',1)
    plot(Traveled,alphax,'k.','markersize',14)
    % plot(alpha,'r.','markersize',12)
end

```

```

if flipper == 1
    figure(9)
    hold on
    plot(Traveled,fliplr(alphax),'r-','linewidth',1.5)
    % plot(alpha,'r-','linewidth',1)
    plot(Traveled,fliplr(alphax),'k.','markersize',14)
    % plot(alpha,'r.','markersize',12)
end

disp('average cross distance')
avgCrossL = mean(CrossL)

clear Ref

```

## APPENDIX E

### MATLAB - Fitting

#### *Contents*

- Traveled,alphax
- Pause
- Normalize section
- Fit to normalized coordinates
- Linear Fitting
- Sqrt Fitting
- Cubic Fitting

#### *Traveled,alphax*

```
if flipper == 0
    alpha_fit = alphax;
end

if flipper == 1
    alpha_fit = fliplr(alphax);
end
```

#### *Pause*

```
figure(10)
hold on
plot(alpha_fit,'r-','linewidth',1)
plot(alpha_fit,'k.','markersize',12)
```

```

pause

XC(1) = input('min? ');
XC(2) = input('max? ');

Normalize section

alpha_i = alpha_fit(XC(1):XC(2));
alpha_i_min = 0; % DO NOT SHIFT ALPHA IT WILL ADD AN X TERM
% alpha_i_min = min(alpha_i);
alpha_i_delta = max(alpha_i)-min(alpha_i);
alpha_n = (alpha_i-alpha_i_min)/alpha_i_delta;

% alpha_i_delta = 0;
% alpha_n = alpha_i;

y_i = Traveled(XC(1):XC(2));
y_i_min = min(y_i);
y_i_delta = max(y_i)-min(y_i);
y_n = (y_i-min(y_i))/y_i_delta;
% y_i_min = 0;

figure(12)
hold on
plot(y_n,alpha_n,'r-','linewidth',1)
plot(y_n,alpha_n,'k.','markersize',12)

```

*Fit to normalized coordinates*

*Linear Fitting*

```
[linear_fit,linear_fit_p] = fit(y_n',alpha_n', 'poly1');

if linear_fit_p.rsquare < .98
    disp('confidence for linear case too low')
else
    figure(12)
    plot(y_n,linear_fit(y_n),'b-','linewidth',2)
    disp('confidence for linear is good')
    new_y = linspace((0 + linear_fit.p2)*y_i_delta,(1 + linear_fit.p2)*y_i_delta,length(y_i))
    fin_alpha = linear_fit.p1/y_i_delta*alpha_i_delta;
    alpha_x_fin=fin_alpha*new_y+alpha_i_min;

    figure(9)
    hold on
    plot(new_y-min(new_y)+y_i(1),alpha_x_fin,'b-','linewidth',2)

    alpha_string = num2str(fin_alpha)
    yo_string = num2str([new_y(1) new_y(end)])
    x1 = y_i(round(.5*length(y_i)));
    y1 = alpha_x_fin(round(.5*length(alpha_x_fin)));
    xly = y_i(round(.4*length(y_i)));
    yly = alpha_x_fin(round(.4*length(alpha_x_fin)));

    %    txt1 = ['\alpha = ' alpha_string];
    %    text(x1,y1,txt1)
```

```

%      txt2 = ['y* = ' yo_string];
%      text(xly,yly,txt2)

finx = meshgrid(linspace(-avgCrossL/2,avgCrossL/2));
finy = meshgrid(linspace(min(new_y),max(new_y)))';
finz = (fin_alpha*finy+alpha_i_min).*finx-follow;
figure(66)
surf(finx,finy,finz)
%      contour(finx,finy,finz)
end

Sqrt Fitting

ft1 = fittype('a*(x+b)^.5','coefficients',{ 'a','b'}); [sqrt_fit,sqrt_fit_p] = fit(y_n,alpha_n',ft1);

if cubic_fit_p.rsquare < .99 disp('confidence for Sqrt case too low') else plot(y_n,cubic_fit(y_n),'g-
','linewidth',2) disp('confidence for Sqrt is good') new_y = linspace((0 + cubic_fit.b)*y_i_delta,(1
+ cubic_fit.b)*y_i_delta,length(y_i)); fin_alpha = cubic_fit.a/y_i_delta^.5*alpha_i_delta;
alpha_x_fin=fin_alpha*new_y.^.5+alpha_i_min;

figure(9)
plot(y_i,alpha_x_fin,'b-','linewidth',1.5)
finx = meshgrid(linspace(-avgCrossL/2,avgCrossL/2));
finy = meshgrid(linspace(min(new_y),max(new_y)))';
finz = (fin_alpha*finy.^.5+alpha_i_min).*finx-follow;
figure(66)
surf(finx,finy,finz)
end

```



### *Cubic Fitting*

```
ft1 = fitttype('a*(x+b)^3','coefficients',{ 'a','b'});
[cubic_fit,cubic_fit_p] = fit(y_n',alpha_n',ft1);

if cubic_fit_p.rsquare < .98
    disp('confidence for cubic case too low')
else
    figure(12)
    plot(y_n,cubic_fit(y_n),'g-','linewidth',2)
    disp('confidence for cubic is good')
    new_y = linspace((0 + cubic_fit.b)*y_i_delta,(1 + cubic_fit.b)*y_i_delta,length(y_i))
    fin_alpha = cubic_fit.a/y_i_delta^3*alpha_i_delta;
    alpha_x_fin=fin_alpha*new_y.^3+alpha_i_min;

    figure(9)
    plot(new_y-min(new_y)+y_i(1),alpha_x_fin,'g-','linewidth',2)

    alpha_string = num2str(fin_alpha)
    yo_string = num2str([new_y(1) new_y(end)])
    x1 = y_i(round(.5*length(y_i)));
    y1 = alpha_x_fin(round(.5*length(alpha_x_fin)));
    xly = y_i(round(.4*length(y_i)));
    yly = alpha_x_fin(round(.4*length(alpha_x_fin)));

    txt1 = ['\alpha = ' alpha_string];
    text(x1,y1,txt1)
    txt2 = ['y* = ' yo_string];
```

```

text(xly,yly,txt2)

finx = meshgrid(linspace(-avgCrossL/2,avgCrossL/2));
finy = meshgrid(linspace(min(new_y),max(new_y)))';
finz = (fin_alpha*finy.^3+alpha_i_min).*finx-follow;
figure(66)
surf(finx,finy,finz)
end

```

## REFERENCES



- Corless, R. M., Gonnet, G. H., Hare, D. E. G., Jeffrey, D. J., & Knuth, D. E. (1996). On the lambertw function. *Advances in Computational Mathematics*, 5(1), 329–359. Retrieved from <http://dx.doi.org/10.1007/BF02124750> doi: 10.1007/BF02124750
- Cushman-Roisin, B., & Beckers, J.-M. (2008). *Introduction to geophysical fluid dynamics*. Academic Press.
- Granger, R. A. (1995). *Fluid mechanics*. Dover.
- Ibanez, R. (2017). *Matlab ocean topography id*. Retrieved from <https://ruyibanez.wordpress.com/bathymetry-solver-and-analytic-sloping-barotropic-flow-solver/>
- Jia Wang, F. J. S., Moto Ikeda. (2003). A theoretical, two-layer, reduced-gravity model for descending dense water flow on continental shelves/slopes. *Journal of Geophysical Research*, 108(C5).
- John, H.-C., Mittelstaedt, E., & Schulz, K. (1998). The boundary circulation along the european continental slope as transport vehicle for two calanid copepods in the bay of biscay. *Oceanologica Acta*, 21(2), 307 - 318. Retrieved from <http://www.sciencedirect.com/science/article/pii/S0399178498800170> doi: [http://dx.doi.org/10.1016/S0399-1784\(98\)80017-0](http://dx.doi.org/10.1016/S0399-1784(98)80017-0)
- Kuehl, J. (2014). An analytic solution for barotropic flow along a variable slope topography. *Geophysical Research Letters*, 41.
- Kuehl, J., & Sheremet, V. (2014). Two-layer gap-leaping oceanic boundary currents: experimental investigation. *Journal of Fluid Mechanics*, 740, 97-113.
- Maier, K. L., Brothers, D. S., Paull, C. K., McGann, M., Caress, D. W., & Conrad, J. E. (2016). Records of continental slope sediment flow morphodynamic responses to gradient and active faulting from integrated {AUV} and {ROV} data, offshore palos verdes, southern california borderland. *Marine Geology*, -. Retrieved from <http://www.sciencedirect.com/science/article/pii/S0025322716302304> doi: <http://dx.doi.org/10.1016/j.margeo.2016.10.001>
- Nguyen, T., Morey, S. L., Dukhovskoy, D. S., & Chassignet, E. P. (2015, 4). Nonlocal impacts of the loop current on crossslope nearbottom flow in the northeastern gulf of mexico. *Geophysical Research Letters*, 42(8), 2926–2933. Retrieved from <http://dx.doi.org/10.1002/2015GL063304> doi: 10.1002/2015GL063304
- Pedlosky, J. (1979). *Geophysical fluid dynamics*. Springer-Verlag.
- Pijush K. Kundu, D. R. D., Ira M. Cohen. (2011). *Fluid mechanics* (fifth ed.). Academic Press.

- Samelson, R., & Wiggins, S. (2000). *Lagrangian transport in geophysical jets and waves*. Springer.
- Zavala, L., & van Heijst, G. (2002). Ekman effects in a rotating flow over bottom topography. *Journal of Fluid Mechanics*, 471, 239-255.